Title

Modeling the effects of diagenesis on carbonate clumped-isotope values in deep- and shallow-water settings

Authors

Stolper, Daniel A
Eiler, John M
Higgins, John A

Publication Date

2018-04-01

DOI

10.1016/j.gca.2018.01.037

Peer reviewed

Available online at www.sciencedirect.com

ScienceDirect

Geochimica et Cosmochimica Acta 227 (2018) 264–291

Geochimica et Cosmochimica Acta

www.elsevier.com/locate/gca

Modeling the effects of diagenesis on carbonate clumped-isotope values in deep- and shallow-water settings

Daniel A. Stolper [a,*], John M. Eiler [b], John A. Higgins [c]

[a] Department of Earth and Planetary Science, University of California, Berkeley, CA 94720, USA
[b] Division of Geological and Planetary Sciences, California Institute of Technology, Pasadena, CA 91125, USA
[c] Department of Geosciences, Princeton University, Princeton, NJ 08544, USA

Received 21 June 2017; accepted in revised form 30 January 2018; available online 09 February 2018

Abstract

The measurement of multiply isotopically substituted ('clumped isotope') carbonate groups provides a way to reconstruct past mineral formation temperatures. However, dissolution-reprecipitation (i.e., recrystallization) reactions, which commonly occur during sedimentary burial, can alter a sample's clumped-isotope composition such that it partially or wholly reflects deeper burial temperatures. Here we derive a quantitative model of diagenesis to explore how diagenesis alters carbonate clumped-isotope values. We apply the model to a new dataset from deep-sea sediments taken from Ocean Drilling Project site 807 in the equatorial Pacific. This dataset is used to ground truth the model. We demonstrate that the use of the model with accompanying carbonate clumped-isotope and carbonate $\delta^{18}O$ values provides new constraints on both the diagenetic history of deep-sea settings as well as past equatorial sea-surface temperatures. Specifically, the combination of the diagenetic model and data support previous work that indicates equatorial sea-surface temperatures were warmer in the Paleogene as compared to today. We then explore whether the model is applicable to shallow-water settings commonly preserved in the rock record. Using a previously published dataset from the Bahamas, we demonstrate that the model captures the main trends of the data as a function of burial depth and thus appears applicable to a range of depositional settings.

Keywords: Carbonate sediments; Clumped isotopes; Diagenesis; Stable-isotope geochemistry

1. INTRODUCTION

The oxygen isotopic composition of carbonate minerals has been used extensively to reconstruct the temperatures of ancient oceans (e.g., Emiliani, 1955; Shackleton and Kennett, 1975; Miller et al., 1987; Zachos et al., 2001). Oxygen isotopes can be used to reconstruct carbonate mineral formation temperatures due to the temperature-dependent partitioning of ^{18}O vs. ^{16}O in carbonate relative to water for systems at thermodynamic equilibrium (e.g., Urey, 1947; McCrea, 1950). $^{18}O/^{16}O$ compositions of carbonates are generally quantified using $\delta^{18}O$ values[1] ($\delta^{18}O_{carb}$).

This approach to determining past carbonate formation temperatures requires isotopic equilibrium to exist between two phases, water and a carbonate mineral such as calcite. Thus, one must know the oxygen isotopic composition of both phases to determine a mineral's formation temperature. Although ancient carbonate minerals are preserved

* Corresponding author at: Department of Earth and Planetary Science, University of California, Berkeley, Berkeley, CA 94720, USA.
E-mail address: dstolper@berkeley.edu (D.A. Stolper).

[1] $\delta = (R_{sample}/R_{standard} - 1) \times 1000$ where $R = [^{13}C]/[^{12}C]$ for carbon isotopes and $[^{18}O]/[^{16}O]$ for oxygen isotopes. For carbon isotopes, samples are referenced to the VPDB scale and for oxygen isotopes, to VSMOW.

https://doi.org/10.1016/j.gca.2018.01.037
0016-7037/

in the rock record over most of Earth's history (Veizer and Mackenzie, 2003), equivalent archives of seawater are not. Consequently, past seawater $^{18}O/^{16}O$ compositions ($\delta^{18}O_{fluid}$ values) must be estimated in order to use $\delta^{18}O_{carb}$ values for most paleotemperature reconstructions. Problematically, estimates and models past seawater $\delta^{18}O_{fluid}$ values are in disagreement by a few to greater than 10 per mil hundreds of millions to billions of years in the past (Muehlenbachs and Clayton, 1976; Gregory and Taylor, 1981; Gregory, 1991; Kasting et al., 2006; Jaffrés et al., 2007), limiting the utility of carbonate $\delta^{18}O$ paleothermometry for many Earth-history questions. For comparison, a 1‰ change in $\delta^{18}O_{carb}$ values at Earth-surface temperatures (e.g., 0–30 °C) but fixed $\delta^{18}O_{fluid}$ is equivalent to an approximately 4–5 °C change in mineral formation temperature (e.g., Kim and O'Neil, 1997).

An alternative approach to $\delta^{18}O_{carb}$-based paleothermometry is the reconstruction of formation temperatures using the distribution of isotopes within carbonate groups. Specifically, the abundance of carbonate groups with more than one rare (generally heavy) isotope (a 'clumped' isotopologue), such as $^{13}C^{16}O_2^{18}O^{2-}$, relative to a random distribution of isotopes amongst all isotopologues is a unique function of temperature for an isotopically equilibrated system. This temperature dependence has been demonstrated for carbonates using theory (Schauble et al., 2006), experiments (e.g., Ghosh et al., 2006; Dennis and Schrag, 2010; Zaarur et al., 2013; Kluge et al., 2015; Defliese et al., 2015; Kelson et al., 2017), and observations of environmental inorganic and biological materials formed at known temperatures (e.g., Ghosh et al., 2007; Tripati et al., 2010; Eagle et al., 2010, 2015; Thiagarajan et al., 2011; Henkes et al., 2013; Grauel et al., 2013; Came et al., 2014; Wacker et al., 2014; Douglas et al., 2014; Kele et al., 2015; Katz et al., 2017). Carbonate clumped-isotope abundances are currently quantified through the measurement of mass 47 CO_2 molecules ($^{13}C^{16}O^{18}O$, $^{12}C^{17}O^{18}O$, and $^{13}C^{17}O_2$) released from carbonate minerals via phosphoric acid digestion (Ghosh et al., 2006). Excesses of mass 47 CO_2 molecules relative to a random distribution of isotopes is expressed by the symbol[2] Δ_{47}. At isotopic equilibrium, Δ_{47} values are monotonic functions of mineral formation temperatures (e.g., Ghosh et al., 2006; Dennis and Schrag, 2010; Zaarur et al., 2013; Kluge et al., 2015; Defliese et al., 2015; Kelson et al., 2017).

Importantly, measurements of Δ_{47} values can be used to reconstruct past formation temperatures of carbonate minerals regardless of the average oxygen isotopic composition of the fluid (including both liquid water and igneous melts) or solid (e.g., in solid-state phase changes) from which the carbonate crystalized — such a reconstruction implicitly assumes the carbonate formed in internal isotopic equilibrium. Indeed, the combination of formation temperatures derived from Δ_{47} values along with $\delta^{18}O_{carb}$ values allows the $\delta^{18}O$ value of the formational fluid or solid to be estimated. This approach has been used to estimate the oxygen-isotopic composition of seawater from which ancient carbonates precipitated (e.g., Came et al., 2007; Finnegan et al., 2011; Petersen and Schrag, 2015; Bergmann et al., 2018).

Use of $\delta^{18}O_{carb}$ and Δ_{47} values to reconstruct past carbonate formation temperatures in the surface ocean implicitly requires that the carbonates being analyzed faithfully record their 'original' isotopic composition established during initial crystallization. However, based on studies of carbonate and pore-fluid Sr, O, Ca, and Mg concentrations and isotopic compositions as well as scanning electron microscopy, it has been demonstrated that deep-sea carbonates can undergo extensive recrystallization (10 s of percent) during burial and lithification over tens of millions of years (Richter and DePaolo, 1987, 1988; Richter and Liang, 1993; Schrag et al., 1995; Pearson et al., 2001; Fantle and DePaolo, 2006, 2007; Higgins and Schrag, 2012; Fantle, 2015). We use the term 'recrystallization' to indicate the reactions that dissolve and reprecipitate minerals with no net change in the overall mass of carbonate mineral (other than removal or addition of trace constituents such as Mg or rare isotopes); i.e., recrystallization is used to discuss diagenetic reactions in which dissolution and reprecipitation rates are equal. We note that other uses of recrystallization sometimes include processes in which carbonate mineralogy is changed such as the conversion of aragonite to calcite or conversion of either to dolomite. This type of recrystallization is often referred to as neomorphism and commonly occurs in shallow-water depositional systems found on continental shelves and slopes (e.g., Brand and Veizer, 1981; Banner and Hanson, 1990; Melim et al., 2001, 2002; Dyer et al., 2017; Higgins et al., 2018).

Here we explore with a quantitative model the effects of dissolution-reprecipitation reactions (i.e., recrystallization) on Δ_{47} values in carbonate sediments during burial and lithification. We first take established mathematical frameworks used to quantify how dissolution-reprecipitation reactions in carbonate sediments affect chemical and bulk isotopic compositions (i.e., $\delta^{18}O$ and $\delta^{13}C$ values) of carbonate minerals (Richter and DePaolo, 1987, 1988; Schrag et al., 1992, 1995; Fantle and DePaolo, 2006; Fantle et al., 2010; Higgins and Schrag, 2012) and extend them to include predictions of how Δ_{47} values change during diagenesis. We compare model results constrained by independent predictions of various boundary conditions (e.g., seawater temperatures, recrystallization rates, and others discussed below) to newly measured carbonate clumped-isotope temperatures at Ocean Drilling Project (ODP) site 807 on the Ontong Java Plateau in the western Pacific Ocean. This exercise demonstrates that the trend of our measured Δ_{47} values vs. depth are well described by previous models of diagenesis. This provides confidence in both the model and the external boundary conditions used. Following this, we explore the model's validity in shallow-water continental shelf settings via comparison of model predictions to previously published data from the Bahamas (Winkelstern and Lohmann, 2016) and show the model is consistent with measurements made on samples from these settings.

[2] $\Delta_{47} = ([^{47}R][^{47}R^*] - 1) \times 1000$ where $^{47}R = [^{13}C^{16}O^{18}O + ^{12}C^{17}O^{18}O + ^{13}C^{17}O_2]/[^{12}C^{16}O_2]$ and * denotes the random distribution.

2. METHODS

2.1. Sample selection and preparation

Archived samples were selected from the ODP site 807 core (Kroenke et al., 1991). This core was taken in the equatorial western Pacific (Fig. A1) and penetrated over 1.3 km of carbonate sediment. Sediment ages range from the quaternary to the Cretaceous and are typically >90% by weight calcium carbonate. The ooze-chalk transition occurs between 252 and 312 meters below the seafloor (mbsf) while the chalk-limestone transition is defined at 1098 mbsf, but lithification to limestone begins at ~850 mbsf (Borre and Fabricius, 1998). Typical sedimentation rates range from 18 to 34 meters per million years. Further information on the core and sedimentary properties can be found in Kroenke et al. (1991).

At Princeton, bulk samples were sieved in methanol into different size fractions including <20, 20–65, 65–250 and >250 μm, air dried, and then shipped to the California Institute of Technology for isotopic measurements. In some cases the samples between 20 and 250 μm in size were combined to make a single size fraction.

2.2. Isotopic measurements

Measurements of carbonate $\delta^{13}C_{carb}$, $\delta^{18}O_{carb}$, and Δ_{47} values were made at the California Institute of Technology. CO_2 was extracted from samples using a phosphoric acid digestion, purified, and introduced to a Thermo-Finnigan 253 isotope-ratio mass spectrometer using an automated acid-digestion and gas-purification device described in Passey et al. (2010). Isotopic ratios were measured following the procedures outlined in Eiler and Schauble (2004), Huntington et al. (2009), and Dennis et al. (2011).

$\delta^{13}C_{carb}$ and $\delta^{18}O_{carb}$ values are reported relative to the VPDB scale and VSMOW respectively based on a previously calibrated gas standard (OzTech). $\delta^{13}C_{carb}$ and $\delta^{18}O_{carb}$ values were calculated based on the isotopic compositions of VSMOW and VPDB given in Santrock et al. (1985). We justify our use of the Santrock et al. (1985) VSMOW and VPDB values in Appendix A.1.

Carbonate $\delta^{18}O$ values were calculated from the measured CO_2 $\delta^{18}O$ values using the isotopic fractionation factor ($^{18}R_{CO3}/^{18}R_{CO2}$) for phosphoric acid digestion at 90 °C of 1.00821 (Swart et al., 1991). Gases equilibrated at 25 °C using water and 1000 °C in quartz-glass tubes were used to place Δ_{47} measurements into the absolute reference frame (Dennis et al., 2011). Δ_{47} values are given in the 25 °C acid-digestion reference frame by assuming a difference between samples digested between 90 and 25 °C of 0.092‰ (Henkes et al., 2013).

Multiple calibrations currently exist for the conversion of Δ_{47} values to clumped-isotope-based temperatures. The dependence of Δ_{47} vs. temperature for these calibrations differs by up to 2x and depends on the laboratory that generated the calibration (Ghosh et al., 2006; Dennis and Schrag, 2010; Dennis et al., 2011; Zaarur et al., 2013; Defliese et al., 2015; Kluge et al., 2015). Although why calibrations differ between laboratories remains uncertain, recent results indicate that standardization protocols using carbonate standards with agreed upon Δ_{47} values can allow different laboratories to converge on a single calibration line (e.g., Daeron et al., 2017). As this work was initiated and completed before any such standardization routine has become widespread, we present our data as measured at Caltech in the absolute reference frame. Isotopic values for standards measured at Caltech are given in Tables S1 and S2. When a unified temperature vs. Δ_{47} calibration is agreed upon, our Δ_{47} data can be cast into that reference frame based on the values for the standards we measured. Critically, it appears that as long as the Δ_{47} values are measured in the same laboratory where the calibration used was generated, then the calculated clumped-isotope temperatures will be correct regardless of any later interlaboratory standardization. Such standardization should translate the Δ_{47} values along with the temperature vs. Δ_{47} calibration of the laboratory to any such interlaboratory reference frame but leave the calculated temperatures unchanged. Thus when discussing our data, we use a temperature calibration generated at the Caltech laboratory. Likewise, when discussing the data of from Winkelstern and Lohmann (2016), we use the Δ_{47} vs. temperature calibration of Defliese et al. (2015), as both the that and calibration were generated in the same laboratory.

We convert our Δ_{47} values to clumped-isotope-based temperatures using calibration data generated in the Caltech laboratory. Specifically we use the calibration of Ghosh et al. (2006) as given in the absolute reference frame by Dennis et al. (2011) to convert Δ_{47} values to apparent clumped-isotope temperatures for samples measured here. Although this calibration is based on the precipitation of inorganic calcite at only 4 distinct temperatures, it has been verified in subsequent studies of biogenic samples with known carbonate formation temperatures measured at Caltech (Ghosh et al., 2007; Came et al., 2007; Eagle et al., 2010, 2015; Tripati et al., 2010; Thiagarajan et al., 2011). To demonstrate this, we compiled previous measurements made at Caltech for samples with known formation temperatures (both inorganic and biogenic) from 1 to 1650 °C in the absolute reference and generated a temperature vs. Δ_{47} calibration (Fig. A2). We compared this calibration to the Ghosh et al. (2006) calibration from 1 to 50 °C. Deviations in Δ_{47} values between the two calibrations from 1 to 50 °C range from −0.004 to +0.01‰, all within the typical precision of Δ_{47} measurements (±0.01‰, 1 standard deviation [σ]). For consistency with previous studies, we use the Ghosh et al. (2006) calibration for our temperature reconstructions from 1 to 50 °C and note that use of a larger complied calibration has no effect on our model or conclusions. Finally, for model calculations when sedimentary temperatures exceed 50 °C, we use the 1–1650 °C calibration created above (Fig. A2) to ensure we are always interpolating between calibrated points for temperature vs. Δ_{47}.

Samples were measured at least 2–3 times with replication occurring in different analytical sessions (except sample

9H3, >250 μm, which was only measured once). An analytical session is defined here as a period of time in which samples and standards were measured continuously and compared to a single set of 1000 °C heated and 25 °C equilibrated gases. These sessions generally lasted ~1–2 weeks. Different analytical sessions for this study are separated in time (typically ~1–2 months) by other analytical sessions in which carbonate samples unrelated to this study were measured.

In all analytical sessions, two standards, a Carrara Marble standard ($n = 43$) and a travertine standard (TV01; $n = 41$) were measured to monitor and evaluate the accuracy and precision of the isotopic measurements between and within sessions. Average $\delta^{18}O_{carb}$ and $\delta^{13}C_{carb}$ values of the standards are both within 0.11‰ of expected values (Table A1). Standard deviations for $\delta^{18}O_{carb}$ and $\delta^{13}C_{carb}$ values of the standards were 0.24 and 0.11‰. This is significantly higher than typical precisions for these analyses: ~0.1‰ for $\delta^{18}O_{carb}$ and 0.05‰ for $\delta^{13}C_{carb}$ (e.g., Stolper and Eiler, 2016). $\delta^{18}O_{carb}$ and $\delta^{13}C_{carb}$ of standards run within a single session show average standard deviations of 0.05‰ and 0.04‰ respectively, indicating the imprecision was due to differences between analytical sessions.

To deal with this, sample $\delta^{18}O_{carb}$ and $\delta^{13}C_{carb}$ values from a given analytical session were corrected based on the average difference between expected vs. observed values for the standards for that session. For example, if standards were on average elevated in $\delta^{18}O_{carb}$ in a given session by 0.1‰, 0.1‰ was subtracted from all samples measured in that analytical session. This follows typical standardization techniques for isotopic measurements (e.g., Coplen et al., 2006). This standardization scheme reduces the pooled standard deviations of all samples from 0.16 and 0.09‰ for $\delta^{18}O_{carb}$ and $\delta^{13}C_{carb}$ values to 0.06‰ and 0.07‰, respectively. Average corrected values for samples are given in Table 1. Individual measurements for all samples are given in Supplementary Table 1.

Average measured Δ_{47} values of both standards are within 0.01‰ of the expected values (Table A2). Standard deviations are 0.011‰ for the Carrara marble standard and 0.016‰ for the TV01 standard. The pooled standard deviation for the samples is 0.012‰. Thus the external reproducibility of Δ_{47} values for samples and standards is similar to the expected counting-statistics-based external precision of the measurement (~±0.01‰). Despite this level of reproducibility, we additionally corrected the Δ_{47} data based on deviations for the standards from their expected values for each analytical session. Specifically, we made our corrections using the observed deviation in the Δ_{47} value of the standard as a linear function of the Δ_{47} value — this is based on the correction scheme given in Thiagarajan et al. (2014). Application of this correction scheme does not change the external precision (the pooled standard deviation for samples remains at 0.012‰), but ensures samples corrected for their bulk isotopic compositions are also corrected for their Δ_{47} values. Average corrected Δ_{47} values for samples are given in Table 1. Uncorrected and corrected Δ_{47} values of every measurement are given in Supplementary Table 2.

3. MODELING DIAGENESIS

3.1. Diagenesis in deep-sea sediments

The effects of diagenesis on the chemical and isotopic composition of deep-sea carbonates has been explored extensively using both numerical models and measurements of the isotopic and chemical composition of carbonates and pore fluids for a variety of elements including oxygen, magnesium, and strontium (Killingley, 1983; Richter and DePaolo, 1987, 1988; Schrag et al., 1992, 1995; Richter and Liang, 1993; Fantle and DePaolo, 2006; Fantle et al., 2010; Higgins and Schrag, 2012). Here, we first review the conceptual and quantitative framework of these models (Section 3.1.1). Then we extend these models to include the effects of diagenesis on Δ_{47} values (Section 3.1.2). Finally we provide illustrative calculations of the effects (both in magnitude and direction) diagenesis can have on Δ_{47} values in deep–sea (Section 3.1.3) and shallow-water (Section 3.2) sediments.

3.1.1. Background for deep-sea sediments

Carbonate sediments in the deep sea (>1000 m depths) today are largely composed of the remnants of organisms (coccolithophores and foraminifera) that live and calcify in the photic zone of the water column (typically the top ~100 m of the water column). As a result, the chemical and isotopic compositions of bulk deep-sea carbonate dominantly reflect the conditions (e.g., temperature) of carbonate formation at or near the sea surface when first deposited on the seafloor (assuming no diagenesis occurs during sinking). During burial and lithification, dissolution-reprecipitation (i.e., recrystallization) reactions occur that can modify the chemical and isotopic composition of sedimentary carbonate. The consequences of diagenesis for the chemical and isotopic composition of carbonates in deep-sea sediment can be significant as the temperature and chemical composition of pore fluids in sedimentary systems can differ from those found in the surface ocean (up to ~50 °C for the first kilometer of burial). For example, diagenetic recrystallization of deep-sea carbonates is thought to have modified many Eocene-Paleocene deep-sea carbonates such that $\delta^{18}O$ values yield surface-water temperatures that are ~10 °C lower than the original formation temperature of the samples (Schrag et al., 1995; Pearson et al., 2001; Kozdon et al., 2011), though see Bernard et al. (2017) for a recent, alternative view on the effects of diagenesis on $\delta^{18}O_{carb}$ values in deep-sea sediments.

Models that describe rates of carbonate diagenesis in deep-sea sediments (e.g., Richter and DePaolo, 1987) generally specify (*i*) the boundary conditions of the system including the temperature and isotopic/chemical composition of the surface ocean, the temperature at the sediment-water interface, and the geothermal temperature gradient in the sediments; (*ii*) The sedimentary deposition and compaction rates; (*iii*) The rates of sediment dissolution and reprecipitation; And (*iv*) the diffusion of dissolved species in the fluids — diffusion within the solid is ignored. All of these parameters are allowed to vary as a function of time.

Table 1
Sample information and isotopic measurements.

Sample name	Size fraction (μm)	Depth (m)	n	$\delta^{18}O$ (‰)[a]	1 s.e.[b]	$\delta^{13}C$ (‰)[c]	1 s.e.[b]	Δ_{47} (‰)[d]	1 s.e.[b]
1H3	<20	3.75	3	29.57	0.02	0.63	0.03	0.711	0.013
1H3	20–65	3.75	3	29.47	0.05	0.05	0.04	0.711	0.004
1H3	65–250	3.75	3	29.67	0.07	0.56	0.06	0.704	0.010
1H3	>250	3.75	3	29.98	0.05	1.16	0.02	0.715	0.007
2H1	<20	8.15	3	29.85	0.04	0.57	0.03	0.713	0.008
2H1	20–65	8.15	3	29.60	0.02	0.11	0.03	0.708	0.010
2H1	65–250	8.15	3	29.54	0.05	0.21	0.09	0.716	0.004
2H1	>250	8.15	3	29.96	0.04	1.47	0.02	0.697	0.004
3H3	<20	19	2	29.87	0.00	0.25	0.04	0.721	0.007
3H3	>250	19	2	30.08	0.01	0.65	0.00	0.727	0.019
4H3	<20	28.5	2	30.18	0.02	-0.06	0.04	0.743	0.008
4H3	>250	28.5	2	30.13	0.01	1.33	0.10	0.724	0.005
7H6	<20	57	3	30.21	0.04	0.31	0.03	0.725	0.004
7H6	20–65	57	3	29.96	0.05	0.17	0.04	0.701	0.008
7H6	65–250	57	3	29.84	0.05	0.49	0.05	0.720	0.007
7H6	>250	57	3	30.01	0.04	1.20	0.04	0.730	0.005
8H3	<20	60	2	30.13	0.01	0.76	0.04	0.730	0.009
8H3	>250	60	2	29.78	0.06	1.64	0.02	0.707	0.021
9H3	<20	76	2	29.91	0.05	0.11	0.04	0.730	0.013
9H3	>250	76	1	29.73	0.00	1.36	0.01	0.709	0.007
12H	<20	103	3	30.72	0.04	0.97	0.02	0.729	0.012
12H	20–65	103	3	30.03	0.04	-0.18	0.02	0.731	0.009
12H	65–250	103	3	29.83	0.05	0.60	0.01	0.706	0.011
12H	>250	103	3	29.77	0.05	0.98	0.19	0.709	0.005
16H3	<20	143	2	30.47	0.02	0.78	0.03	0.716	0.024
16H3	>250	143	2	30.37	0.03	0.84	0.02	0.712	0.002
24H3	<20	218	2	30.69	0.02	1.36	0.02	0.725	0.008
24H3	>250	218	2	30.44	0.13	1.49	0.05	0.724	0.019
27H3	<20	248	2	31.19	0.05	1.49	0.04	0.726	0.019
27H3	>250	248	2	31.02	0.06	1.56	0.02	0.715	0.017
32×2	<20	295	2	30.62	0.03	1.36	0.03	0.739	0.007
32×2	>250	295	2	30.65	0.05	1.34	0.04	0.732	0.007
46-6	<20	435	3	30.77	0.08	2.26	0.03	0.709	0.002
46-6	20–250	435	3	30.46	0.05	1.84	0.03	0.737	0.004
46-6	>250	435	3	30.84	0.04	2.07	0.04	0.740	0.005
55×5	<20	50	3	31.06	0.02	1.78	0.01	0.730	0.000
55×5	20–250	50	3	30.52	0.02	1.10	0.01	0.714	0.003
55×5	>250	50	3	31.03	0.01	1.54	0.00	0.722	0.010
75-3	<20	712	3	30.68	0.02	1.85	0.13	0.723	0.006
75-3	20–250	712	3	30.83	0.05	1.74	0.09	0.724	0.005
75-3	>250	712	3	30.72	0.03	1.71	0.01	0.730	0.003
02R-1	Bulk	790	3	30.67	0.02	1.49	0.02	0.730	0.004
25R-1	Bulk	948	3	29.80	0.03	2.09	0.03	0.711	0.009
52R2	Bulk	1172	5	28.63	0.02	3.26	0.01	0.704	0.015

[a] Referenced to the VSMOW scale. Values corrected based on measured values of in-house standards.
[b] ±1 standard error
[c] Referenced to the VPDB scale. Values corrected based on measured values of in-house standards.
[d] Given in the absolute reference frame (ARF) of Dennis et al. (2011). Values corrected based on measured values of in-house standards.

These models also assume carbonate that forms in the sediment column (i.e., that is diagenetic in origin), forms in isotopic equilibrium with the co-occurring pore fluids. This assumption is supported by inferred rates of carbonate precipitation in deep-sea sediments ($\sim 10^{-19}$ mol/m^2/sec; Fantle and DePaolo, 2007), which is orders of magnitude lower than previously estimated rates ($\sim 10^{-12}$ mol/m^2/sec) required to form carbonate minerals in carbon, oxygen, and clumped isotopic equilibrium with water regardless of the temperature or pH of the system (Watkins et al., 2013, 2014; Watkins and Hunt, 2015).

The model we use to quantify the effects of diagenesis on $\delta^{18}O_{carb}$ and Δ_{47} values is based on the 1-D advection-reaction-diffusion model developed by Richter and DePaolo (1987). This model was originally used to describe changes in strontium concentrations and isotopic ratios ($^{87}Sr/^{86}Sr$) of carbonates and pore fluids during burial. It was later extended to include the effects of diagenesis on $\delta^{18}O_{carb}$ and $\delta^{18}O_{H2O}$ values in Schrag et al. (1992). Full descriptions of the model framework are given in those studies. However, for completeness, key procedural steps of the model are reviewed here: First, sediment with defined

initial thickness and porosity is added to a preexisting sediment column. Second, sediment 'boxes' below this newly added box are compacted (causing upward advection of pore fluids) and new thicknesses and porosities for each box are calculated. Third, all sediment boxes then undergo recrystallization at a model-defined rate, which is a function of sediment age (see below). Note that recrystallization in a box neither adds nor subtracts any mass such that total dissolution matches total reprecipitation at all times (thus conserving mineral and fluid masses during recrystallization). As a result, recrystallization in this model does not cause any changes in physical sediment properties (e.g., porosity). At this point, the model returns to the first step and continues.

Sedimentation rates are estimated using sedimentary ages (generally constrained by biostratigraphy) vs. depth below the seafloor. Compaction rates are estimated using the porosity profile in the sediments (e.g., Richter and DePaolo, 1987). Following previous model formulations, recrystallization rates, as a percent of the carbonate recrystallized per unit time, given by R, are assumed to decrease exponentially as a function of the age of the sediment. The equation used has the following form:

$$R(t) = \alpha_{rx} + \beta_{rx} e^{-t/\gamma_{rx}} \quad (1)$$

where t is time, and α_{rx} (‰/myr), β_{rx} (‰/myr), and γ_{rx} (myr^{-1}) are constants. α_{rx}, β_{rx}, and γ_{rx} can be estimated using strontium concentrations and isotopic compositions ($^{87}Sr/^{86}Sr$ ratios) in pore fluids and sediments (Richter and DePaolo, 1987, 1988; Richter and Liang, 1993; Schrag et al., 1995). Note that we also use α below as the symbol for isotopic fractionation factors. Rather than change the symbols used in past studies, we use subscripts for α for clarity.

3.1.2. Recrystallization and $\delta^{18}O_{carb}$ in deep-sea sediments

Modeling the effects of diagenesis on $\delta^{18}O_{carb}$ values requires knowing the $\delta^{18}O_{carb}$ values of newly deposited carbonate sediments. This in turn requires knowledge of the temperature history and $\delta^{18}O_{fluid}$ history of surface seawater and the temperature-dependent fractionation factor between the carbonate mineral and water ($\alpha_{carb\text{-}H2O}$). $\alpha_{carb\text{-}H2O}$ is defined as follows:

$$\alpha_{carb-H_2O} = \frac{[^{18}O]_{carb}/[^{16}O]_{carb}}{[^{18}O]_{H_2O}/[^{18}O]_{H_2O}} = \frac{1000 + \delta^{18}O_{carb}}{1000 + \delta^{18}O_{H_2O}} \quad (2)$$

where square brackets denote concentrations. We note that $\alpha_{carb\text{-}H2O}$ values can vary as a function of parameters other than temperature including carbonate growth rates and solution pH (e.g., McCrea, 1950; Kim and O'Neil, 1997; Zeebe, 1999; Dietzel et al., 2009; Watkins et al., 2014) and organism-specific effects (i.e., 'vital effects') if the carbonate is biogenic in origin (e.g., Erez, 1978; Weiner and Dove, 2003). However, in past models, only the temperature-dependent effect has been considered (Schrag et al., 1995). As discussed above, this assumption is likely acceptable for carbonates formed during diagenesis given the slow rates of recrystallization.

The temperature dependence of $\alpha_{carb\text{-}H2O}$ is taken from Watkins et al. (2013) as given in Fig. 6 of that study and equation 19 of Watkins et al. (2014). We use this $\alpha_{carb\text{-}H2O}$ calibration as it expresses the fractionation factor for carbonate formation at sufficiently slow rates that the oxygen isotopes of carbonate and water are in equilibrium. For site 807 discussed below, the same $\alpha_{carb\text{-}H2O}$ vs. temperature calibration appears to describe the initial and diagenetic carbonate $\delta^{18}O_{carb}$ values equally well.

The isotopic composition of diagenetic carbonate that is incorporated into the sediment during dissolution-reprecipitation reactions is controlled by sedimentary temperatures and pore-fluid $\delta^{18}O_{fluid}$ values as a function of sediment depth and age. Sedimentary temperatures are found by specifying the temperature history at the sediment water interface (i.e., the temperature of bottom oceanic waters) and the sedimentary geothermal gradient. Following previous models (e.g., Schrag et al., 1995; Schrag, 1999), we assume that pore-fluid $\delta^{18}O_{fluid}$ values at the sediment-water interface are identical to bottom-water values and that no gradient between surface and deep-water $\delta^{18}O_{fluid}$ values exists. We note that differences between surface and deep water $\delta^{18}O_{fluid}$ values do exist — for example today, $\delta^{18}O_{fluid}$ values of equatorial waters over the Ontong Java are elevated by ~0.6‰ relative to deep Pacific waters (Craig and Gordon, 1965; LeGrande and Schmidt, 2006). As knowledge of this difference is poor over Earth's history, we assume surface and deep waters were identical, which is in accordance with previous studies (e.g., Schrag et al., 1995; Schrag, 1999).

Finally, in previous models (e.g., Schrag et al., 1995; Schrag, 1999), pore fluid $\delta^{18}O$ values were assumed to have a constant depth gradient based on observations of pore fluids from a variety of deep-sea cores. We follow that assumption here as well. A review of the processes controlling sedimentary pore fluid compositions in deep-sea sediments is given in Lawrence and Gieskes (1981).

The change in the $\delta^{18}O_{carb}$ value of a sedimentary box can be described by the following equation:

$$\frac{d\delta^{18}O_{carb}(t,d)}{dt} = \Big[-R(t) \times \delta^{18}O_{carb}(t,d) + R(t)\Big(\Big[1000 + \delta^{18}O_{H_2O,\,pore\,fluid}(t,d)\Big]\alpha_{carb-H_2O}(T) - 1000\Big)\Big], \quad (3)$$

where $\delta^{18}O_{carb}(t,d)$ is the oxygen isotopic composition of the sedimentary box undergoing diagenesis at time t and depth d; $R(t)$ is the recrystallization rate of that box at time t; $\delta^{18}O_{H2O,\ pore\ fluid}(t, d)$ is the isotopic composition of the pore fluid in contact with that box; and $\alpha_{carb\text{-}H2O}(T)$ is the oxygen isotope fractionation factor between carbonate and water at temperature T. We note that formulating the problem in this manner makes the typical assumption that $\delta^{18}O$ values can be treated as analogous to the concentration of ^{18}O in the various phases (Criss, 1999).

This equation can be rewritten in the following manner:

$$\frac{d\delta^{18}O_{carb}(t,d)}{dt} = \Big[-R(t) \times \delta^{18}O_{carb}(t,d) + R(t) \times \delta^{18}O_{carb,\,diagenetic}(t,d)\Big]. \quad (4)$$

Here, $\delta^{18}O_{carb,\ diagenetic}$ is the isotopic composition of the carbonate formed in sedimentary column and added to the box. For a given time step, dt, the model removes $[R(t) \times dt]$ percent of the original carbonate and replaces it with $[R(t) \times dt]$ percent diagenetic carbonate. Thus the total mass of carbonate in a box remains constant. The density of the box changes due to loss of porosity via pore-fluid advection during compaction.

We do not develop equations that track the isotopic composition of the fluids as the gradient describing the oxygen isotopic composition of the pore fluid, as discussed above, is assumed to be constant (Schrag et al., 1995; Schrag, 1999). The relevant equations that describe the isotopic evolution of the fluid are given in Schrag et al. (1992).

3.1.3. Extension of the diagenetic model to Δ_{47} values for deep-sea sediments

The extension of the diagenetic model to include Δ_{47} values involves the incorporation of no additional free parameters. This is because Δ_{47} values are defined solely by a sample's formation temperature (for a phase formed in isotopic equilibrium). Temperature histories for (*i*) the surface ocean, (*ii*) the sediment-water interface, and (*iii*) within the sediment column are necessarily prescribed by any diagenetic model that describes $\delta^{18}O_{carb}$ values. Consequently, any model that seeks to describe the effects of diagenesis on $\delta^{18}O_{carb}$ values during burial necessarily predicts the Δ_{47} value of carbonates undergoing burial and diagenesis as well. Δ_{47} values can thus serve to independently test models of carbonate diagenesis based on $\delta^{18}O_{carb}$ values.

Carbonate formed in pore fluids can have Δ_{47}, $\delta^{18}O_{carb}$, and $\delta^{13}C_{carb}$ values different from the bulk sediment undergoing recrystallization. When this diagenetic carbonate is added to the bulk sediment, the Δ_{47} value of this sediment will not necessarily represent a weighted average (by carbonate weight percent) of Δ_{47} values of the original and newly added carbonate. Specifically, non-linear Δ_{47} mixing effects occur when the $\delta^{18}O$ and $\delta^{13}C$ of end members differ substantially (~10 s of per mil; Eiler and Schauble, 2004; Affek and Eiler, 2006; Defliese and Lohmann, 2015). Non-linear mixing effects for Δ_{47} values often can be neglected in models of diagenesis (e.g., Stolper and Eiler, 2016) where the $\delta^{13}C$ value of the diagenetic and original carbonate components do not differ substantially regardless of the $\delta^{18}O_{carb}$ value of the carbonate added during diagenesis. In Appendix A.2, we demonstrate that such an assumption is acceptable when modeling diagenesis at site 807. Thus, we do not explicitly model changes in pore-fluid $\delta^{13}C$ values and the effects of recrystallization on bulk carbonate $\delta^{13}C$ values.

Under the assumption that Δ_{47} values mix linearly during diagenesis in deep-sea carbonate sediments, we can express the rate-of-change of Δ_{47} of carbonate undergoing recrystallization as follows:

$$\frac{d\Delta_{47,carb}(t,d)}{dt} = \left[-R(t) \times \Delta_{47,\ carb}(t,d) + R(t) \times \Delta_{47,\ carb\ diagenetic}(t,d)\right]. \quad (5)$$

Here $\Delta_{47,\ carb}$ (t, d) is the Δ_{47} value of the sedimentary carbonate undergoing diagenesis and $\Delta_{47,\ carb\ diagenetic}$ (t, d) is the Δ_{47} of the diagenetic carbonate formed in the sedimentary column. For all examples below, the Δ_{47} vs. temperature calibration of Ghosh et al. (2006) is used (translated into the absolute reference frame in Dennis et al. (2011)).

3.1.4. Illustrative examples of the diagenetic model in deep-sea sediments

Here we examine two end-member examples commonly seen in deep-sea settings — this follows the sorts of examples given in Schrag et al. (1992) for the effects of diagenesis on $\delta^{18}O_{carb}$ values. In the first example, carbonate forms at 30 °C in the upper water column and then falls to the seafloor. We assume a seafloor temperature of 0 °C, which is within the range of modern and glacial deep-water temperatures (−2 to +3 °C; Adkins et al., 2002) (Fig. 1A–F). This example illustrates what occurs in typical modern low-latitude deep-sea sediments. In the second example, surface waters and the seafloor are both held at 0 °C, mimicking modern high-latitude environments; Fig. 2A–F).

For all examples, we assume no compaction occurs, that calcium carbonate accumulates at a rate of 20 m per million years and that a constant geotherm of 30 °C/km exists. Compaction is critical for relating the depth of sediments to the age of the sediments in the model as well as for diagenetic problems that involve the explicit modeling of pore-fluid compositions. As we are not modeling changes in pore-fluid compositions nor are we matching a specific age-depth relationship, compaction can be (and is) ignored for the examples explored here. We assume the $\delta^{18}O_{fluid}$ value of the ocean is constant at 0‰ and that pore fluid $\delta^{18}O_{fluid}$ values are constant with depth and identical to seawater. Finally, we assume the following recrystallization parameter values: $\alpha_{rx} = 0.2$ (%/myr), $\beta_{rx} = 6$ (%/myr), and $\gamma_{rx} = 5$ (myr). These values are typical of values used in previous models of bulk sedimentary recrystallization (Richter and Liang, 1993). We do not vary the temperature histories of the surface or bottom water temperatures of the ocean for these examples.

For systems in which carbonates form initially at 30 °C and begin diagenesis at 0 °C, $\delta^{18}O_{carb}$ values increase by 1.7‰ over the first 500 m of burial (Fig. 1A and B). Below 500 m, $\delta^{18}O_{carb}$ values do not change significantly. Note, this is not because recrystallization has stopped. Rather, the $\delta^{18}O_{carb}$ value of the diagenetic end member and the sedimentary values are sufficiently similar such that the $\delta^{18}O_{carb}$ value of the recrystallizing sediment does not change over this depth interval. Δ_{47} values also increase over the first 500 m by 0.04‰ (Fig. 1C and D), equivalent to a decrease in clumped-isotope-based temperatures of 8 °C (Fig. 1E and F) and then reach stable values — again this is not because recrystallization has ceased, but is instead due to similarities in sedimentary and diagenetic carbonate Δ_{47} values over this depth range. As typical precisions of Δ_{47} measurements (at 1 standard error) range

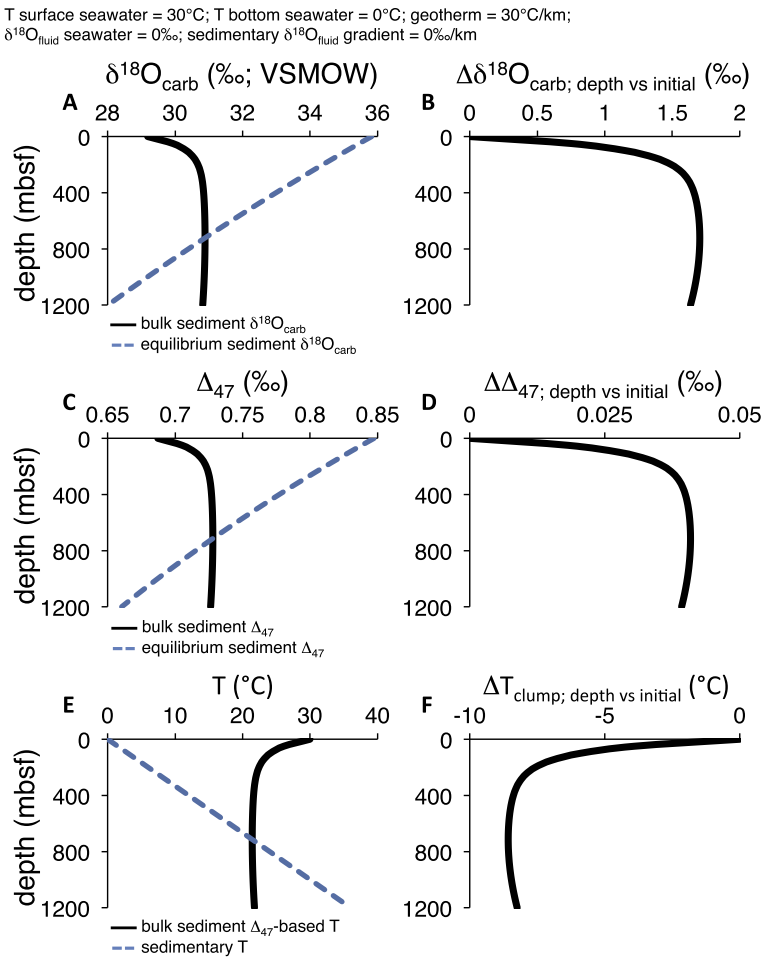

Fig. 1. Model examples of the effects of dissolution-reprecipitation reactions on carbonate $\delta^{18}O_{carb}$, Δ_{47}, and Δ_{47}-based temperatures for an equatorial deep-sea setting. Surface temperatures are 30 °C. Deep-water temperatures are 0 °C. The geothermal gradient is 30 °C/km. $\delta^{18}O_{fluid}$ value of seawater and the pore fluids are 0‰. Black lines are the bulk carbonate sediment values. Dashed blue lines are the values in the sediment column. In (B), (D), and (F) the change (Δ) between the measured and initial value of the bulk carbonate as a function of depth is given. See Section 3.1.4 for more details.

from ±0.01 to 0.02‰, this change should be analytically resolvable. We note that our modeled $\delta^{18}O_{carb}$ results are in agreement with previous illustrative models on the effects of diagenesis on $\delta^{18}O_{carb}$ values (Schrag et al., 1992).

In contrast, when surface and deep-ocean temperatures are similar (in our example 0 °C), smaller changes in $\delta^{18}O_{carb}$ and Δ_{47} values are observed. For our example, $\delta^{18}O$ values decline by 0.6‰ over the first 1200 m of burial (Fig. 2A and B). Δ_{47} values decline by 0.015‰ (Fig. 2C and D), which yields an increase of 2.5 °C for equivalent Δ_{47}-based temperatures (Fig. 2E and F). Δ_{47} precisions of ±0.005‰ (1 s.e.) are possible with replicate analysis (Thiagarajan et al., 2011), but such differences would be challenging to resolve given typical precisions of ±0.01–0.02‰. Again, the $\delta^{18}O_{carb}$ model results are in agreement with previous models on the effects of diagenesis on $\delta^{18}O_{carb}$ values (Schrag et al., 1992).

A general result from these models is that the larger the difference between carbonate formation and initial burial temperatures (i.e.. sediment-water interface temperatures), the larger the overall change in the isotopic composition of the bulk sediment over the first ~1 km of burial. For the examples discussed above, the recrystallization rates are identical and decline with depth with an e-folding length scale of 100 m for the β_{rx} term in Eq. (1). For this reason, most of the recrystallization is concentrated in the ~top 200 m of the sediment column. For the low-latitude example, this depth interval is where the difference between formational and diagenetic temperatures is at a maximum. This results in larger diagenetic changes in both $\delta^{18}O_{carb}$ and Δ_{47} values with depth for low-latitude systems relative to the high-latitude example where formational and burial temperatures are more similar over the first 200 m of burial. In Fig. A3, we provide examples of model calculations for variations in reaction rate, depositional rate, and the sedimentary geotherm.

3.2. Diagenesis in shallow sediments

Carbonates from ancient shallow-water (e.g., shelf) settings commonly yield apparent Δ_{47}-based temperatures greater than 40 °C. Such temperatures are often considered

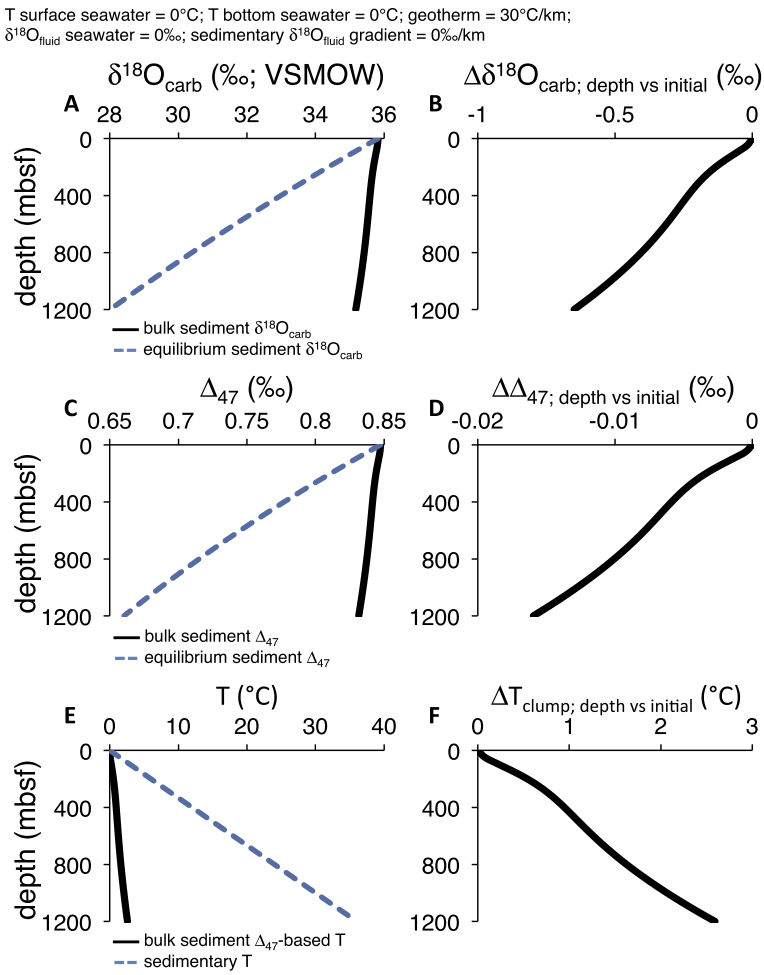

Fig. 2. Model examples of the effects of dissolution-reprecipitation reactions on carbonate $\delta^{18}O_{carb}$, Δ_{47}, and Δ_{47}-based temperatures for a high-latitude deep-sea setting. Surface and deep-sea temperatures are 0 °C. The geothermal gradient is 30 °C/km. $\delta^{18}O_{fluid}$ value of seawater and the pore fluids are 0‰. Black lines are the bulk carbonate sediment values. Dashed blue lines are the values in the sediment column. In (B), (D), and (F) the change (Δ) between the measured and initial value of the bulk carbonate as a function of depth is given. See Section 3.1.4 for more details.

too warm to represent Earth-surface conditions (e.g., Came et al., 2007; Eiler, 2011; Finnegan et al., 2011; Stolper and Eiler, 2016; Winkelstern and Lohmann, 2016), at least over the Phanerozoic. A common explanation for some of these elevated temperatures is that they are the result of dissolution-reprecipitation reactions occurring during sedimentary burial at elevated temperatures. Additionally, solid-state isotope-exchange reactions can also result in changes in Δ_{47} values for samples that reach burial temperatures greater than ~100 °C for calcite (Passey and Henkes, 2012; Henkes et al., 2014; Stolper and Eiler, 2015; Shenton et al., 2015). In this section, we explore the predictions of the model developed for deep-sea sediments for shallow-water systems.

3.2.1. Model considerations for shallow sediments

Before applying the deep-sea diagenetic model to shallower systems, we first consider whether such an extension is appropriate. Shallow-water sediments differ from deep-water settings in a variety of ways. For example, in shallow-water sediments, advection of fluids can occur in the top 10 s of meters, effectively flushing out diagenetically modified fluids with seawater (Swart, 2000); Glacial-interglacial sea-level changes can expose shallow-water sediments to meteoric fluids (Melim et al., 2001); And rapid changes in mineralogy (aragonite to calcite) can occur in the top 100–200 m of such sediments (Melim et al., 2002).

Another difference between shallow- and deep-water settings is that shallow water settings can contain significant (weight percent) concentrations of organic carbon, or, during low-stands, experience flushing of fluids with dissolved inorganic carbon derived from the respiration of organic carbon (Swart and Kennedy, 2012). Both processes can influence the $\delta^{13}C$ values of total dissolved inorganic carbon in pore fluids. For example total dissolved inorganic carbon in the top 100 m of submerged carbonates in the Bahama Banks platform are commonly ~5‰ lower in $\delta^{13}C$ than bulk carbonate at equivalent depths (Kramer et al., 2000; Swart and Eberli, 2005). However, by ~400 mbsf, $\delta^{13}C$ value of dissolved inorganic carbon and carbonate minerals at a given depth are typically within 1‰ of each other, and thus close to being in isotopic equilibrium

(calcite ~1‰ greater in $\delta^{13}C$ than disolved inorganic carbon; Zeebe and Wolf-Gladrow, 2001). Consequently, although diagenetic processes in the top hundred meters below the seafloor in shallow-water carbonate platforms can affect $\delta^{13}C_{carb}$ values, the carbon isotopes are stabilized at greater depths.

Importantly, the processes discussed above are restricted to the top ~400 m of the sedimentary column. For shallow-water systems, the temperature difference between the depositional and diagenetic temperatures over this depth range are 10 °C for a typical 25 °C/km geothermal gradient. As seen in the example of diagenesis in deep-sea sediments in which the formation and initial diagenetic temperatures are identical and the geothermal gradient is 30 °C/km (Fig. 3), diagenesis has a limited effect on Δ_{47}-based temperatures in the first few hundred meters of burial: ~1 °C over the first 400 m.

Thus, these processes, though important for understanding the diagenetic history of platform carbonates (Higgins et al., 2018), are unlikely to have a significant effect on Δ_{47}-based temperatures as they are restricted to the top ~400 m of burial. Rather, the problem of interest here is whether slower rates of recrystallization matter at significant depths (>1000 mbsf), in which burial and formation temperatures diverge by more than 25 °C, for the interpretations of clumped-isotope-based temperatures of ancient carbonates formed in shallow water settings. As $\delta^{13}C$ values between dissolved inorganic carbon and carbonates are similar at these depths (>~400 mbsf), we assume Δ_{47} values mix linearly and use Eq. (5) to describe the effects of diagenesis on Δ_{47} values. Further discussion of this is given Appendix A.2.

3.2.2. Model predictions for shallow-water sediments

We model the effects of diagenesis in shallow sediments using the same general model formulation as described in Section 3.1. Given the potential effects of meteoric diagenesis in the top ~500 m of the sediment column, we do not attempt to model changes in $\delta^{18}O_{carb}$, but instead focus on Δ_{47} values, which are insensitive to the $\delta^{18}O_{fluid}$ value of pore fluids. We assume for this exercise constant sea-surface temperatures of 25 °C (a typical tropical sea-surface temperature) and that bottom water temperatures are identical to sea-surface temperatures (i.e., 25 °C). We assume a 25 °C/km geotherm (a typical value for continental settings). We use a constant depositional rate of 20 m/myr (i.e., the same as for the deep-sea example above). We show the output of the model to depths of 3 km, i.e., to burial temperatures of ~100 °C. We choose this temperature cut off as, for calcite, the influence of solid-state isotope-exchange reactions on clumped-isotope compositions becomes increasingly important to consider at burial temperatures above 100 °C (Passey and Henkes, 2012; Henkes et al., 2014; Stolper and Eiler, 2015; Shenton et al., 2015). For this calculation, we use the Δ_{47} vs. temperature calibration constrained from 1 to 1650 °C (Fig. A2) as discussed in Section 2.2.

We use Eq. (1) to describe the recrystallization rate. We use $\beta_{rx} = 6$ (‰/myr), and $\gamma_{rx} = 5$ (myr), which are the same as those used in section 3.1 for deep-sea diagenesis. The choice of these parameters is relatively unimportant for Δ_{47} values of diagenetically modified platform carbonates. We run the model with three different constant background recrystallization rates [α_{rx}] of 0.1, 0.5, and 1‰/myr. These

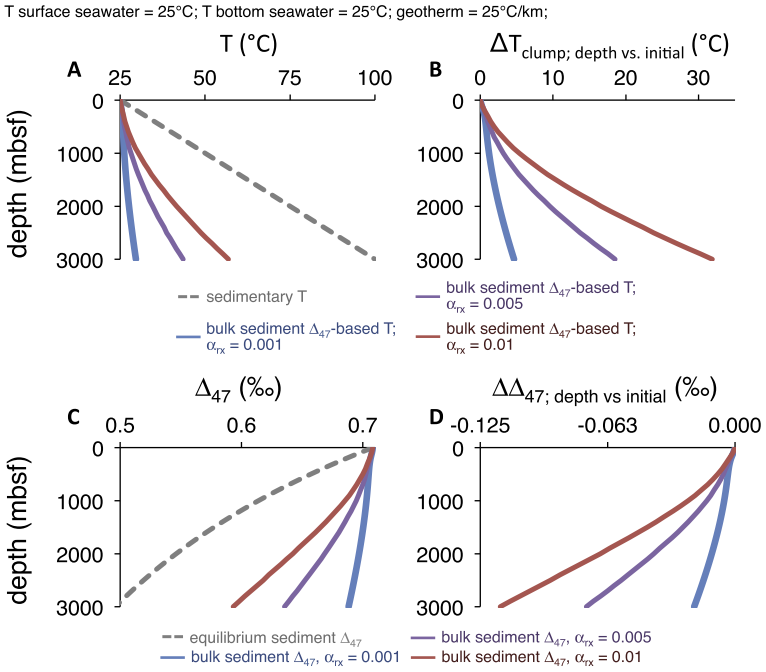

Fig. 3. Model examples of the effects of dissolution-reprecipitation reactions on carbonate Δ_{47}, and Δ_{47}-based temperatures for a shallow sedimentary example. Surface and deep-sea temperatures are 25 °C. The geothermal gradient is 25 °C/km. Dashed grey lines are the values in the sediment column. In (B) and (D), the change (Δ) between the measured and initial value of the bulk carbonate as a function of depth is given. α_{rx} refers to the background reaction rate in the sedimentary column. See section 3.2.2 for more details.

values are within the range of α_{rx} values used in previous models (Richter and Liang, 1993; Schrag et al., 1995; Schrag, 1999).

Model outputs are given in Fig. 3. Δ_{47}-based temperatures change between 1 and 5 °C over the first kilometer of burial. This is despite significant amounts of recrystallization occurring over the first kilometer, 32–55% total recrystallization depending on the chosen rate of background recrystallization rate [α_{rx} in Eq. (1)]. The reason for this relatively small change in Δ_{47} despite extensive recrystallization is that most of this recrystallization is localized in the top few hundred meters of the sediment column where the differences between bulk carbonate Δ_{47}-based temperature and the diagenetic end member are less than 10 °C. This is similar to the case for both $\delta^{18}O_{carb}$ and Δ_{47} values that occurs in deep-sea settings at high latitudes where surface and deep waters have similar temperatures (e.g., Fig. 2; Schrag et al., 1992, 1995).

In the model, α_{rx} values of 0.1 %/myr result in relatively small changes in Δ_{47} values and Δ_{47}-based temperatures over the first 3 km of burial: Δ_{47} values decrease by 0.02‰, equivalent to an increase in 5 °C. Background recrystallization rates of 0.5–1‰/myr result in significantly larger changes in Δ_{47} values with depth, especially below 1 km. Specifically, for α_{rx} values of 0.5 and 1 %/myr, Δ_{47} values decrease by 0.07‰ and 0.115‰ respectively. This is equivalent to an increase in clumped-isotope-based temperatures of 19 and 32 °C respectively.

4. CARBONATE SAMPLES FROM THE EQUATORIAL PACIFIC, OCEAN DRILLING PROJECT SITE 807

4.1. Site 807 description

Carbonate samples from the equatorial western Pacific spanning the Cenozoic were measured for $\delta^{18}O_{carb}$, $\delta^{13}C_{carb}$, and Δ_{47} values. Samples were selected from cores drilled at ODP site 807 (Fig. A1). This site was chosen, in part, because it has been used in numerous previous studies on the effects of diagenesis on the concentrations and isotopic composition of strontium (Fantle and DePaolo, 2006), calcium (Fantle and DePaolo, 2007), and magnesium (Higgins and Schrag, 2012) in carbonates and pore fluids as well as $\delta^{18}O_{carb}$ values (Schrag et al., 1995). All diagenetic models imply substantial amounts of recrystallization occurred at site 807. Specifically, estimates of total percent recrystallization from 0 to 1000 m core depth vary from 35% (Fantle and DePaolo, 2006) to 90% (Schrag et al., 1995). For comparison, the illustrative model (Section 3.1) described above yields 40% total recrystallization by 1000 m depth.

In the context of the end-member diagenetic scenarios discussed in Section 3.1, site 807 is representative of a low-latitude example site in which carbonates form at elevated temperatures in the surface ocean and are initially diagenetically altered at lower temperatures in sediments. Specifically, the surface waters above site 807 in the Western Pacific Warm Pool are ~30 °C today while deep waters in the area are about 2 °C (Locarnini et al., 2006). Based on the illustrative models in Section 3.1, such environments are expected to yield measureable changes in both $\delta^{18}O_{carb}$ (~2‰) and Δ_{47} (~0.04‰) values during burial.

4.2. Site 807 $\delta^{18}O_{carb}$ values

Site 807 $\delta^{18}O_{carb}$ values from foraminifera and bulk sediments have been measured previously (Prentice et al., 1993; Corfield and Cartlidge, 1993; Schrag et al., 1995). $\delta^{18}O_{carb}$ values from other Ontong Java Plateau deep-sea drilling cores are also available (Tripati et al., 2014; Fig. 4A). $\delta^{18}O_{carb}$ values of bulk sediments from the Ontong Java plateau, as discussed in Schrag et al. (1995), are thought to have been modified substantially by diagenetic recrystallization during burial. Specifically, bulk sedimentary $\delta^{18}O_{carb}$ values increase by ~1.5‰ over the first 200 m of the core (Fig. 4A). This increase in $\delta^{18}O_{carb}$ over the first 200 m of the sediment column is consistent with the expected effects of diagenesis on carbonates formed at elevated temperatures (30 °C), undergoing diagenesis in colder bottom waters (e.g., Fig. 1A and B; Schrag et al., 1992, 1995). $\delta^{18}O_{carb}$ values are stable from 200–800 m, but then decrease below 800 m. The background recrystallization rate (0.5 %/myr — α_{rx} in Eq. (1)) used by Schrag et al. (1995) is insufficient to cause this decrease below 800 m for estimated geothermal gradients at this site (25–35 °C/km). Instead, this decrease was attributed to a warmer (2–6 °C) surface ocean temperatures in the Paleogene relative to today (Schrag et al., 1995; Schrag, 1999).

Handpicked foraminifera from site 807 have also been measured (Prentice et al., 1993). The foraminiferal data are generally offset to lower $\delta^{18}O_{carb}$ values than the bulk sediment (Fig. 4A). There appears to be a smaller increase in foraminiferal $\delta^{18}O_{carb}$ values with depth vs. in bulk sediments: Deeper foraminiferal samples (>440 mbsf) are elevated in $\delta^{18}O$ by 0.2‰ relative to the shallower samples (<10 mbsf) compared to the ~1.5‰ increase seen in the bulk sediment over the same depth range. One possibility is that this difference is the result of slower dissolution/reprecipitation kinetics for foraminifera vs. bulk sediment (or at least for the picked samples). Alternatively, temporal changes in vital effects of foraminifera carbonate precipitation (with older foraminifera having have a smaller $\alpha_{CO3\text{-}H2O}$ values than younger foraminifera) could be masking a diagenetic shift in $\delta^{18}O_{carb}$ values. This is returned to below.

In Fig. 4B, $\delta^{18}O_{carb}$ values of the different sedimentary size fractions measured here are compared to previously measured $\delta^{18}O_{carb}$ values. Measured $\delta^{18}O_{carb}$ values of the different size fractions follow a similar trajectory vs. depth as those for bulk sediments from previous studies. Specifically, $\delta^{18}O_{carb}$ values increase by ~1–1.5‰ over the first 200 m, are approximately constant from 200 to 800 m, and then decrease at depths greater than 800 m.

Generally, $\delta^{18}O$ values are ~0.5‰ on average lower for all samples measured in this study (regardless of size fraction) as well as for bulk carbonate samples measured in Tripati et al. (2014; excluding picked foraminifera) as compared to values given for bulk carbonate samples from previous studies (Corfield and Cartlidge, 1993; Schrag et al., 1995). We are unsure of the cause of the difference, but it

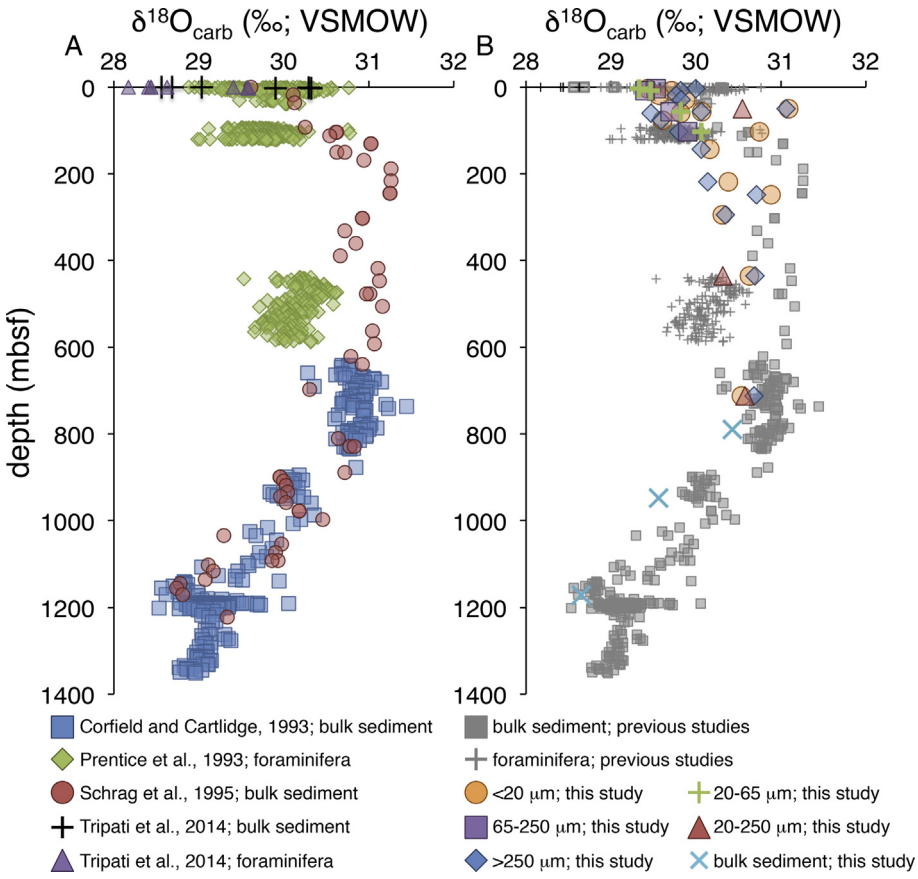

Fig. 4. (A) Previously measured $\delta^{18}O_{carb}$ values of bulk sediment and picked foraminifera from site 807 (Corfield and Cartlidge, 1993; Prentice et al., 1993; Schrag et al., 1995) and nearby sites (Tripati et al., 2014). (B) $\delta^{18}O_{carb}$ values for various size fractions of carbonate sediments measured in this study and compared to previous measurements.

does not impact any interpretations or models described below.

Critically, the isotopic compositions of all size fractions behave in a similar manner and follow similar trajectories as the bulk sediment as a function of depth below the seafloor. Based on this, we propose that the diagenetic recrystallization rates that describe the bulk sediment are applicable to all size fractions. Interestingly, larger size fractions would generally be expected to react more slowly than smaller size fractions based on their lower surface area to volume ratios. However, pelagic foraminifera, which generally make up the bulk of the >250 μm size, are known to have high surface area/volume ratios due to their specific shell morphologies (Pearson et al., 2001). Thus, despite larger overall volumes, planktonic foraminifera may react at rates similar to smaller size fractions. This would indicate that the differences in $\delta^{18}O_{carb}$ between foraminifera and bulk sediments discussed above are largely related to temporal changes in $\alpha_{CO3\text{-}H2O}$ of the picked foraminifera.

4.3. Site 807 $\delta^{13}C_{carb}$ values

Site 807 $\delta^{13}C_{carb}$ values vary from −0.2 to 3.3‰, with higher values observed deeper in the core. We compared the site 807 data to compilations of $\delta^{13}C_{carb}$ from other ODP cores over the Cenozoic (Zachos et al., 2001). These compiled records are derived from benthic foraminifera. Benthic organisms generally have lower $\delta^{13}C_{carb}$ values than surface dwelling organisms due to the respiration of organic carbon in the deep ocean — today, this respiration lowers the $\delta^{13}C$ of dissolved inorganic carbon in the deep ocean by ~1‰ relative to dissolved inorganic carbon the surface ocean (Kroopnick, 1985). To directly compare the site 807 data set to the global compilation, we subtracted 0.95‰ from the $\delta^{13}C_{carb}$ values of the site 807 data, which is the current difference between shallow and deep waters in the equatorial Pacific (Kroopnick, 1985). The two data sets are compared in Fig. 5. This comparison shows that the relative size of changes in site 807 $\delta^{13}C_{carb}$ values tracks global changes in deep-ocean dissolved inorganic $\delta^{13}C$ values over the Cenozoic. Based on this, we interpret the site 807 $\delta^{13}C_{carb}$ values to have been largely unaffected by diagenesis and to reflect, dominantly, $\delta^{13}C$ values of the global dissolved inorganic pool through time. This is in accord with the typical assumption that carbonate carbon isotopes are more difficult to modify during diagenesis than oxygen isotopes due to the lower amounts of carbon vs. oxygen in fluids relative to carbonate sediments (e.g., Banner and Hanson, 1990).

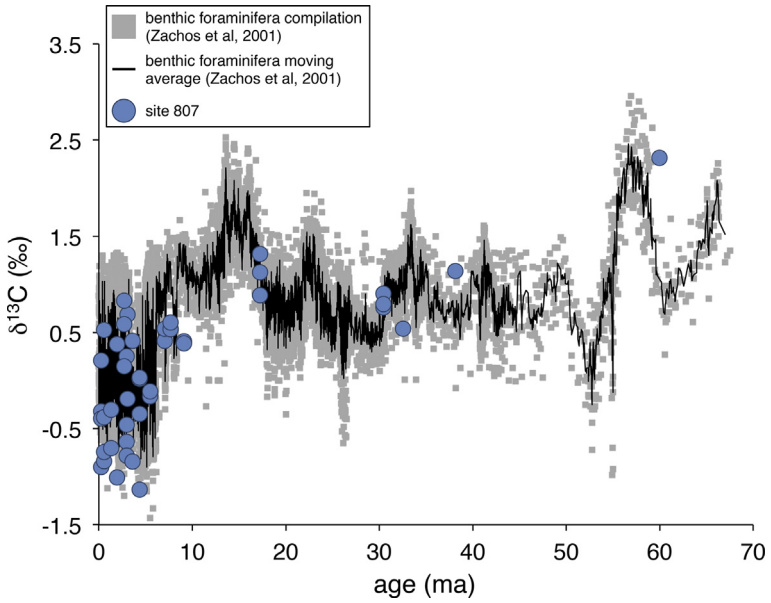

Fig. 5. Site 807 carbonate $\delta^{13}C$ values vs. those measured in other deep-sea cores for benthic foraminifera. Site 807 data are derived dominantly from planktonic organisms. To compare the two records, we lowered site 807 $\delta^{13}C$ values by 0.95‰, which is the current difference in $\delta^{13}C$ between surface and deep water values in the western Pacific Ocean (Kroopnick, 1985). Sediment ages are derived from the age model given in Kroenke et al. (1991).

4.4. Site 807 Δ_{47} values and Δ_{47}-based temperatures

Δ_{47} values vs. depth are shown in Fig. 6A. We include here additional measurements from Tripati et al. (2014) for samples less than 20,000 years old from nearby Ontong Java Plateau sites. Δ_{47} values of samples range from 0.690 to 0.743‰ and show a similar pattern vs. depth as the $\delta^{18}O_{carb}$ values. Specifically, Δ_{47} values increase over the first ~200 m, are approximately constant from 200 to 800 mbsf, and then decrease below 800 m. Measured Δ_{47}-based temperatures range from 19 to 29 °C.

As was the case for $\delta^{18}O_{carb}$ values, no clear differences in overall trends for the different size fractions are apparent. The relationship between Δ_{47} and $\delta^{18}O_{carb}$ values is shown in Fig. 7. Δ_{47} and $\delta^{18}O_{carb}$ values are linearly and positively correlated ($r^2 = 0.56$). Such a positive correlation is what would be expected both for formation as a function of precipitation temperature and for the effects of diagenesis on $\delta^{18}O_{carb}$ and Δ_{47} values in the context of the model presented above. For reference, in Fig. 7, the expected slopes for the equilibrium relationship between water and carbonate are given for waters with $\delta^{18}O_{fluid}$ values of −1, 0, and +1‰. This is the approximate range of values expected for ocean waters over the entire Cenozoic (Shackleton and Kennett, 1975; Miller et al., 1987; Adkins et al., 2002). The data generally follow the trend expected for the generation of carbonates in isotopic equilibrium with water, but there is complexity with this given the presence of both vital effects during precipitation of biogenic sediments and the effects of diagenesis.

Temperatures of surface waters overlying the Ontong Java Plateau (part of the Western Pacific Warm Pool water mass) have ranged between 24 and 30 °C over the past 12 million years, with temperatures typically 2–4 °C warmer in the past 12 million years relative to today (Zhang et al., 2014). Additionally, Paleogene equatorial surface water temperatures are thought to have been warmer than modern waters (up to ~35–40 °C; Pearson et al., 2001; Bijl et al., 2009; Kozdon et al., 2011). Thus, Δ_{47}-based temperatures below 24 °C are unlikely to represent original carbonate formation temperatures and instead likely indicate the occurrence of dissolution-reprecipitation reactions.

The shallowest samples (<10 mbsf) range in Δ_{47}-based temperature from 24 to 30 °C, with an average temperature of 26 ± 0.4 °C (1 s.e.). All samples in this depth range are above expected minimum surface temperatures (based on Mg/Ca and organic proxy thermometry) for the past 2 million years (de Garidel-Thoron et al., 2005; Zhang et al., 2014). Consequently, the Δ_{47}-based temperatures of these shallow (<10 mbsf) samples are consistent with limited diagenesis occurring over this depth range. From 10 to 900 mbsf, samples have Δ_{47}-based temperatures that range from 18.5 to 27 °C, with an average value of 22 °C ± 0.3 (1 s.e.). Thus, Δ_{47}-based temperatures over this depth range (10 to 900 mbsf), are generally cooler than would be expected (<24 °C) based on independent constraints of Cenozoic equatorial surface water temperatures. At depths greater than 900 mbsf, Δ_{47}-based temperatures return to elevated values and are on average 26 ± 0.7 °C (1 s.e.). Thus, the pattern of Δ_{47} vs. depth and Δ_{47}-based temperature vs. depth follow the predicted trajectory given by the illustrative model for carbonates forming in warm surface waters and then undergoing diagenesis in cooler waters in deep-sea sediments (Fig. 1C and E).

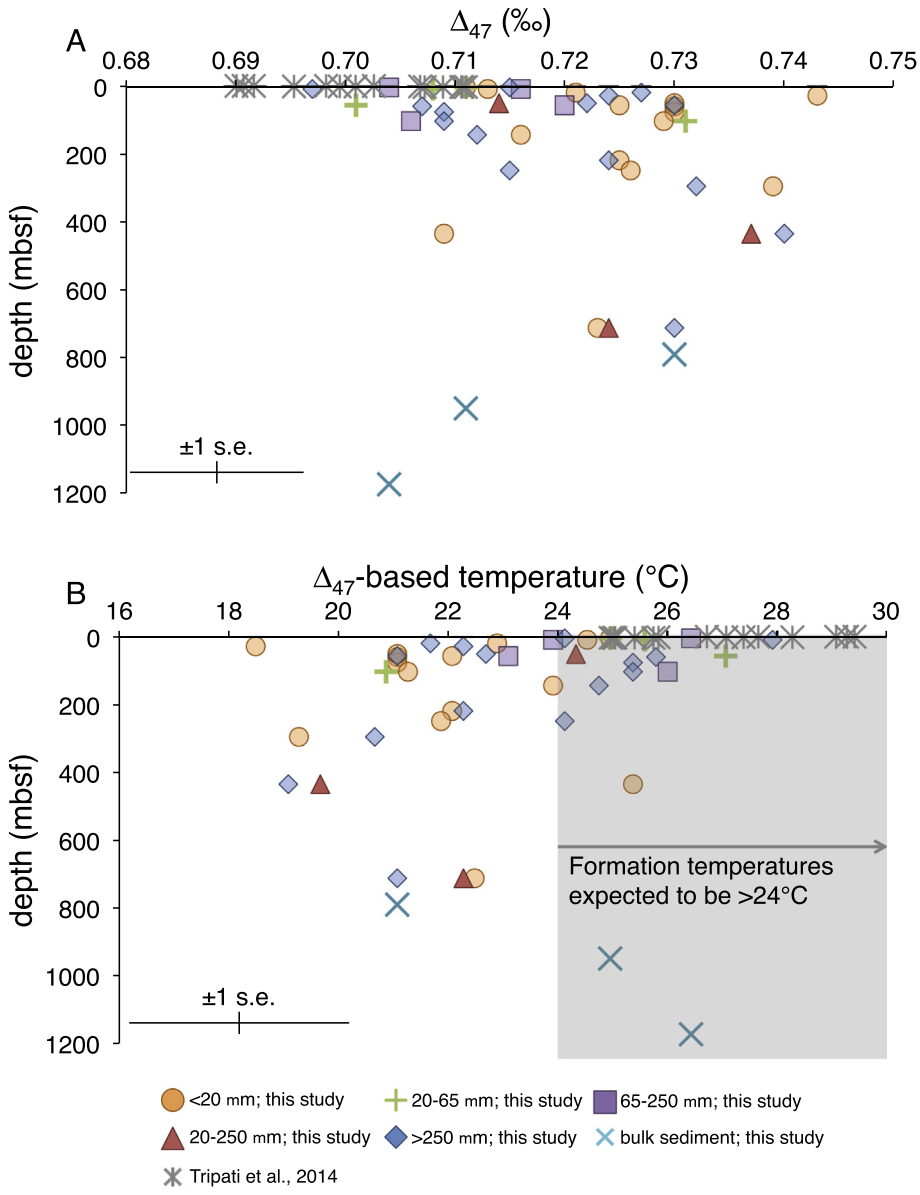

Fig. 6. Clumped-isotope compositions and temperatures measured in this study and in Tripati et al. (2014). (A) Δ_{47} values vs. depth. (B) Measured Δ_{47}-based temperatures. Based on previous reconstructions of equatorial sea-surface temperatures (Pearson et al., 2001; de Garidel-Thoron et al., 2005; Bijl et al., 2009; Kozdon et al., 2011; Zhang et al., 2014), original formation temperatures of all samples are expected to have been >24 °C. Therefore samples with Δ_{47}-based temperatures <24 °C have likely been altered by diagenesis. Typical ±1 s.e. error bars are given for the Δ_{47} measurements and Δ_{47}-based temperatures.

5. MODELING SITE 807 $\delta^{18}O_{CARB}$ AND Δ_{47} DATA

Application of the diagenetic model described in Section 3 to the site 807 data requires prescribing the following potentially time-varying parameters over the course of the Cenozoic: seawater $\delta^{18}O_{fluid}$ values; western Pacific surface-water temperatures; deep-ocean temperatures; the sedimentary geothermal gradient; sediment deposition rates; sediment compaction rates; and sediment recrystallization rates. We used as many independent estimates and constraints on these parameters as possible such that the single free parameter in our modeling efforts is sea-surface temperatures in the Pacific over the Cenozoic. We now describe the bases of the prescribed parameters. A summary is given in Table 2.

5.1. Site 807 model parameters

5.1.1. Cenozoic history of ocean $\delta^{18}O$ values and deep-water temperatures

We used the Cenozoic history of ocean $\delta^{18}O_{fluid}$ values and bottom-water temperatures from Lear et al. (2000). The temperatures are derived from Mg/Ca ratios of benthic foraminifera. $\delta^{18}O$ values of bottom waters are calculated using the formation temperatures derived from the Mg/Ca ratios and $\delta^{18}O_{carb}$ values of benthic foraminifera.

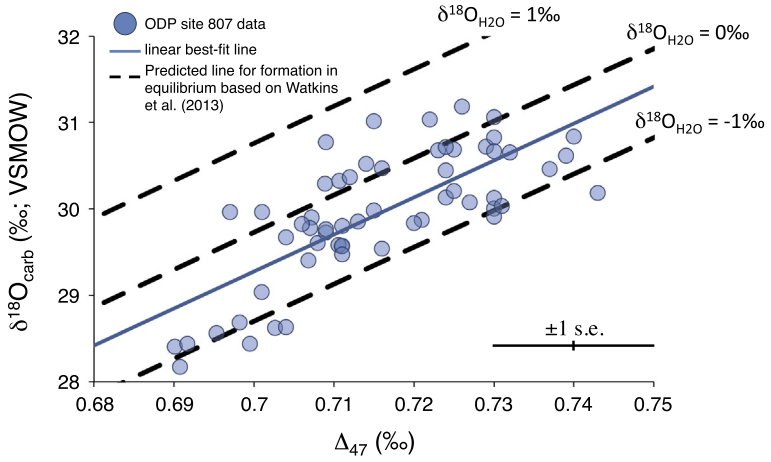

Fig. 7. $\delta^{18}O_{carb}$ vs. Δ_{47} values. Lines for oxygen isotopic equilibrium between calcite and water for waters ranging from −1 to +1‰ (i.e., the ~range expected over the Cenozoic; Shackleton and Kennett, 1975; Miller et al., 1987; Adkins et al., 2002) are also given along with the best-fit line through the data. We note that points with Δ_{47} values below 0.705‰ typically plot below the trend line. This is because these points are dominantly derived from picked foraminifera that precipitated their calcite with $\delta^{18}O$ values lower than that for measured bulk sediment (Tripati et al., 2014).

Table 2
Site 807 model assumptions.

Parameter	Value	Basis	Study
Deep-ocean temperature	Varies with time from ~14 to 1 °C	Mg/Ca measurements of bethic foraminifera	Lear et al. (2000)
Ocean $\delta^{18}O$ value	Varies with time from ~−1 to +0.5‰	Benthic foraminifera $\delta^{18}O_{carb}$ + Mg/Ca measurements	Lear et al. (2000)
Deposition rate	22 m/myr	Site 807 age model	Kroenke et al. (1991)
Compaction rate	Varies with sediment depth	Site 807 porosity data	Higgins and Schrag (2012)
Geothermal gradient	30 °C/km	Estimate	Schrag et al. (1995)
Pore-fluid $\delta^{18}O$ gradient	0 ‰/km	Measurement	Elderfield et al. (1982)
Recrystallization rate	$\alpha_{rx} = 0.5$ %/myr, $\beta_{rx} = 7$ %/myr, $\gamma_{rx} = 9$ myr	Estimate	Schrag et al. (1995)
Ocean surface temperature	Free parameter	–	–

We explored alternative histories of seawater $\delta^{18}O$ and deep-water temperature (Schrag et al., 1995; Cramer et al., 2011) and found differences were negligible and do not effect our conclusions. This is because, to first order, these histories are similar.

5.1.2. Rates of sediment deposition and compaction

Depositional rates were derived from the age model for site 807 given in Kroenke et al. (1991) and are about 22 m/million years on average. Following Higgins and Schrag (2012) we assumed constant depositional rates over the Cenozoic at site 807. Compaction rates were derived from the porosity data following methods outlined in Higgins and Schrag (2012).

5.1.3. Recrystallization rates

Recrystallization rates for site 807 were taken from Schrag et al. (1995) and are the same as those used in that study to model the effects of diagenesis on $\delta^{18}O_{carb}$ data from this site. Specifically, $\alpha_{rx} = 0.5$ (%/myr), $\beta_{rx} = 7$ (%/myr), and $\gamma_{rx} = 9$ (myr) [see equation (1)]. We comment on the chosen values for these recrystallization rates in Appendix A.3.

5.1.4. Sedimentary geothermal gradients

We assumed that the geothermal gradient is constant at 30 °C/km. This is the average value used for the site in Schrag et al. (1995). We chose not to vary this parameter with time as done in Schrag et al. (1995) from 35 to 25 °C/km over the Cenozoic as that this had no noticeable effect on the results.

5.1.5. Sedimentary pore-fluid $\delta^{18}O$ values

The change in $\delta^{18}O_{fluid}$ values with depth is assumed to have a slope of 0 ‰/km (i.e., no change with depth). This differs from the assumed value of this slope of −3 ‰/km used in Schrag et al. (1995), a representative average for deep-sea sediments used in their model for all sites examined. The number we used here (0 ‰/km) is derived from direct measurements of pore fluid $\delta^{18}O_{fluid}$ values in Ontong Java plateau sediments (Elderfield et al., 1982) from Deep-Sea Drilling Program sites 288 and 289. Specifically, samples from ranging 130–940 mbsf yield a slope of

0.4 ± 0.5 (1σ) ‰/km, and thus are indistinguishable at the 1σ level from no change with depth. Elderfield et al. (1982) attributed the constancy of pore-fluid $\delta^{18}O$ values to the buffering effects of extensive recrystallization rates of carbonates on pore-fluid oxygen isotope compositions.

5.2. Modeling Δ_{47} and $\delta^{18}O_{carb}$ values at site 807: The importance of sea-surface temperatures

The temperature history of surface waters from the western equatorial Pacific is less well constrained. Some studies indicate that surface-water temperatures have remained roughly constant over the past 5 million years (Wara et al., 2005), while others have indicated a progressive cooling of about 2 °C from about 6 million years to present (Zhang et al., 2014). We are unaware of any surface temperature reconstructions at this site (or nearby areas) going back more than the past 12 million years (Zhang et al., 2014). Thus, we treat surface temperature as the *sole free parameter* to explore in the model.

Paleolatitude reconstructions of the Ontong Java plateau indicate that site 807 has been within 10° of the equator for the past 50 million years (Chandler et al., 2012). It is generally thought that past equatorial temperatures were equal to or warmer on average than they are today, aside from glacial/interglacial variations (Pearson et al., 2001; Wara et al., 2005; Bijl et al., 2009; Kozdon et al., 2011; Zhang et al., 2014). This provides a first-order constraint on potential past surface seawater temperatures.

Following previous work on $\delta^{18}O_{carb}$ data (Schrag et al., 1995; Schrag, 1999), we do not attempt to find a formal 'best-fit' surface-ocean temperature history for the Pacific Ocean based on the Δ_{47}- and $\delta^{18}O_{carb}$-based temperatures. Instead use the data to explore the plausibility of previously suggested scenarios for surface ocean temperatures over the Cenozoic.

Following Schrag et al. (1995), we first assumed that surface water temperatures above site 807 have remained constant over the Cenozoic. We allowed surface temperatures to range from 24 to 30 °C. This is the range given by Pacific surface-temperature reconstructions over the past 12 million years (de Garidel-Thoron et al., 2005; Zhang et al., 2014; Tripati et al., 2014). Comparison of the model to the $\delta^{18}O_{carb}$ and Δ_{47} datasets (including previously published values) shows agreement for $\delta^{18}O_{carb}$ and Δ_{47} values and Δ_{47}-based temperatures over the past ~40 million years (Fig. 8). However, for older samples (deeper than ~800 mbsf), both Δ_{47} values and $\delta^{18}O_{carb}$ values are consistently lower than predicted by the model. Schrag et al. (1995) and Schrag (1999) noted this disagreement as well in their site 807 $\delta^{18}O_{carb}$ data and in data from other ODP sites for similarly aged samples. They proposed that elevated equatorial surface ocean temperatures of between 2 and 6 °C from 40 to 60 million years ago explains the disagreement.

The deeper $\delta^{18}O_{carb}$ and Δ_{47} can be accommodated by assuming that oceans 65 million years ago were warmer than today at the equator. To illustrate the effects of warmer equatorial temperatures on the model, we assumed that surface equatorial Pacific waters cooled from 36 to 27 °C from 65 to 30 million years ago and then remained constant at 27 °C from 30 million years ago to today. This change causes the model to yield lower $\delta^{18}O_{carb}$ and Δ_{47} values and higher Δ_{47}-based temperatures between 65 and 30 million years ago that visually better match the data (especially the Δ_{47} values) over this time interval (Fig. 9). Given that site 807 has been near the equator (within 10° paleolatitude) over Cenozoic (Chandler et al., 2012), any cooling can be attributed to changes in equatorial temperatures as opposed to migration of site 807 out of the equatorial ocean.

Consequently, the Δ_{47} data, in the context of the diagenetic model, is consistent with proposals for warmer equatorial surface temperatures in the Paleogene. For example, Eocene surface tropical temperatures are estimated to have been at least 32–33 °C based on $\delta^{18}O_{carb}$ values of well preserved foraminifera (Pearson et al., 2001; Kozdon et al., 2011). Organic proxies based on archaeal lipid structures have indicated that equatorial surface water temperatures ranged from 35 to 40 °C in the Eocene (Bijl et al., 2009).

We note, however, that there are alternative model parameterizations that are consistent with the data. For example, increased geothermal gradients or increased deep sedimentary recrystallization rates could also be called on to fit the deeper data (>800 mbsf) without invoking enhanced equatorial surface seawater temperatures. We discuss the choice of recrystallization rate in section A3. Importantly, the model parameters were chosen using independent constraints. Thus the success of the model to describe the Δ_{47} data provides supports not only that accuracy of the model itself, but also past reconstructions of seawater temperatures, ocean $\delta^{18}O_{fluid}$ values, etc.

6. DIAGENESIS AND Δ_{47} VALUES IN SHALLOW-WATER SETTINGS: AN EXAMPLE FROM THE BAHAMAS

The Δ_{47} data presented above for site 807 provide independent evidence for the accuracy of the description of rates of recrystallization in deep sea sediments formulated in Richter and DePaolo (1987) and Richter and DePaolo (1988) and as specifically applied for site 807 for oxygen isotopes in Schrag et al. (1995). When the model is applied to shallow water sediments it indicates that potentially large shifts (>0.1‰) in Δ_{47} values could be observed as samples are buried a few kilometers in depth (Fig. 3C and D).

A key question is whether the model captures what actually occurs in natural shallow-water settings and especially whether diagenesis continues at depths greater than 1 km. To study this, we compared the model to a dataset from Winkelstern and Lohmann (2016), which reports Δ_{47} values from calcite and dolomite samples taken from a drill core through carbonate shelf sediments from Andros Island, Bahamas spanning a depth range of 0 to 4500 m We note that models of diagenesis similar to those used here to describe the exchange of oxygen isotopes between carbonate and pore fluids from 0 to 1100 mbsf in Bahama Bank ODP cores have been applied previously (Swart, 2000). This supports the extension of the diagenetic model to this particular system. However, we note that models of this

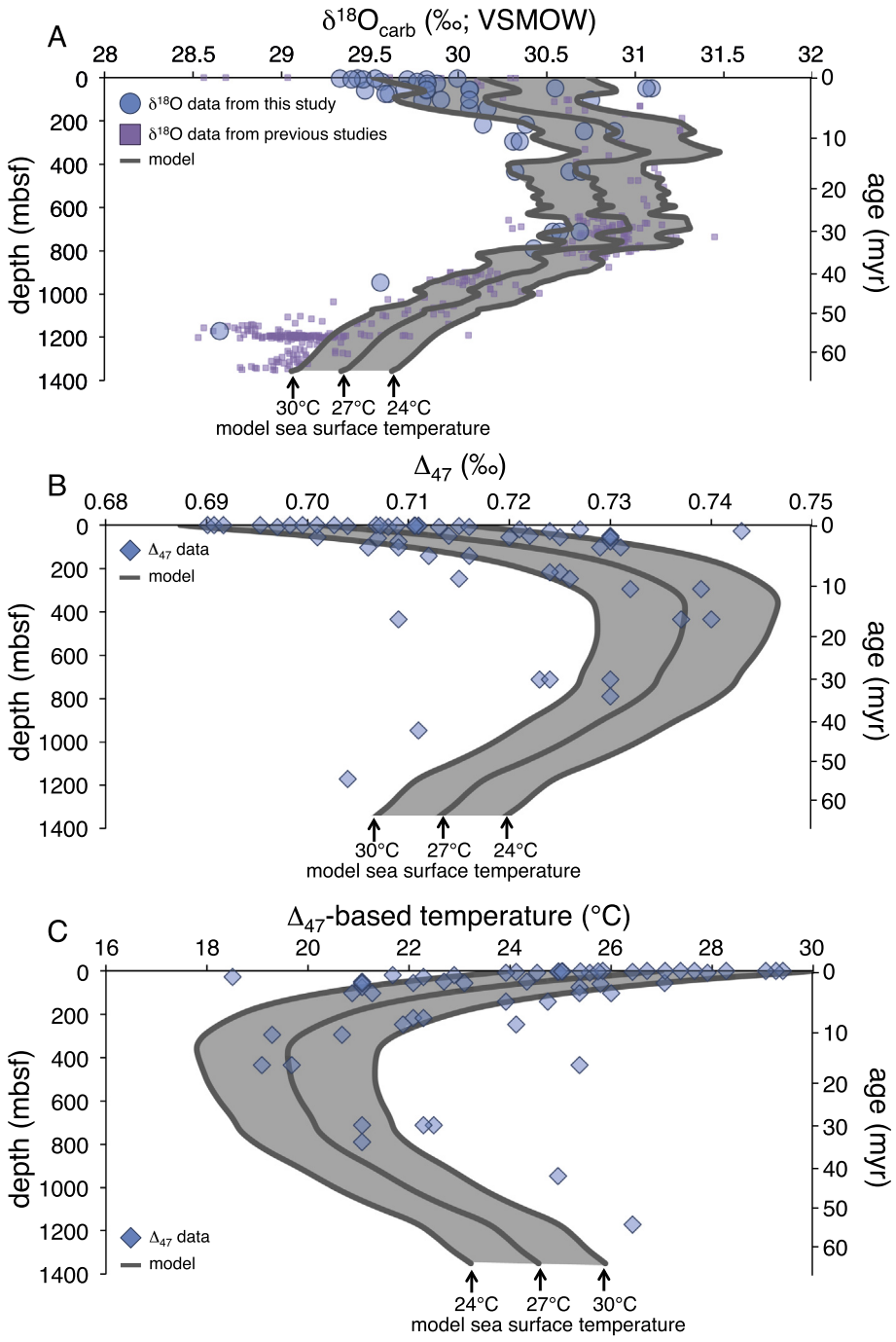

Fig. 8. Comparison of the diagenetic model to site 807 data. For the model, we have assumed constant sea-surface temperatures of 24, 27, and 30 °C, which are the range of temperatures observed for equatorial sea-surface temperatures in the area of study. Agreement between the model and data is apparent for samples <40 Ma (<800 mbsf).

sort are not widely used in the interpretation of diagenesis in shallow-water systems.

Based on information given in Winkelstern and Lohmann (2016), we took the average depositional rate of the system to be 33 m/myr and ran the model for 142 million years. Due to a lack of constraints, we assumed the same porosity vs. depth relationship as site 807. The porosity profile is important for modeling mass transfer between boxes via diffusion and compaction. We are not modeling diffusional processes here, so the precise porosity profile is unimportant for our results.

We assumed constant sea-surface and sediment-water interface temperatures of 27 °C, which is the average surface-water temperature in the area today (Winkelstern and Lohmann, 2016). We assumed a geothermal gradient of 30 °C based on observations of ODP geothermal

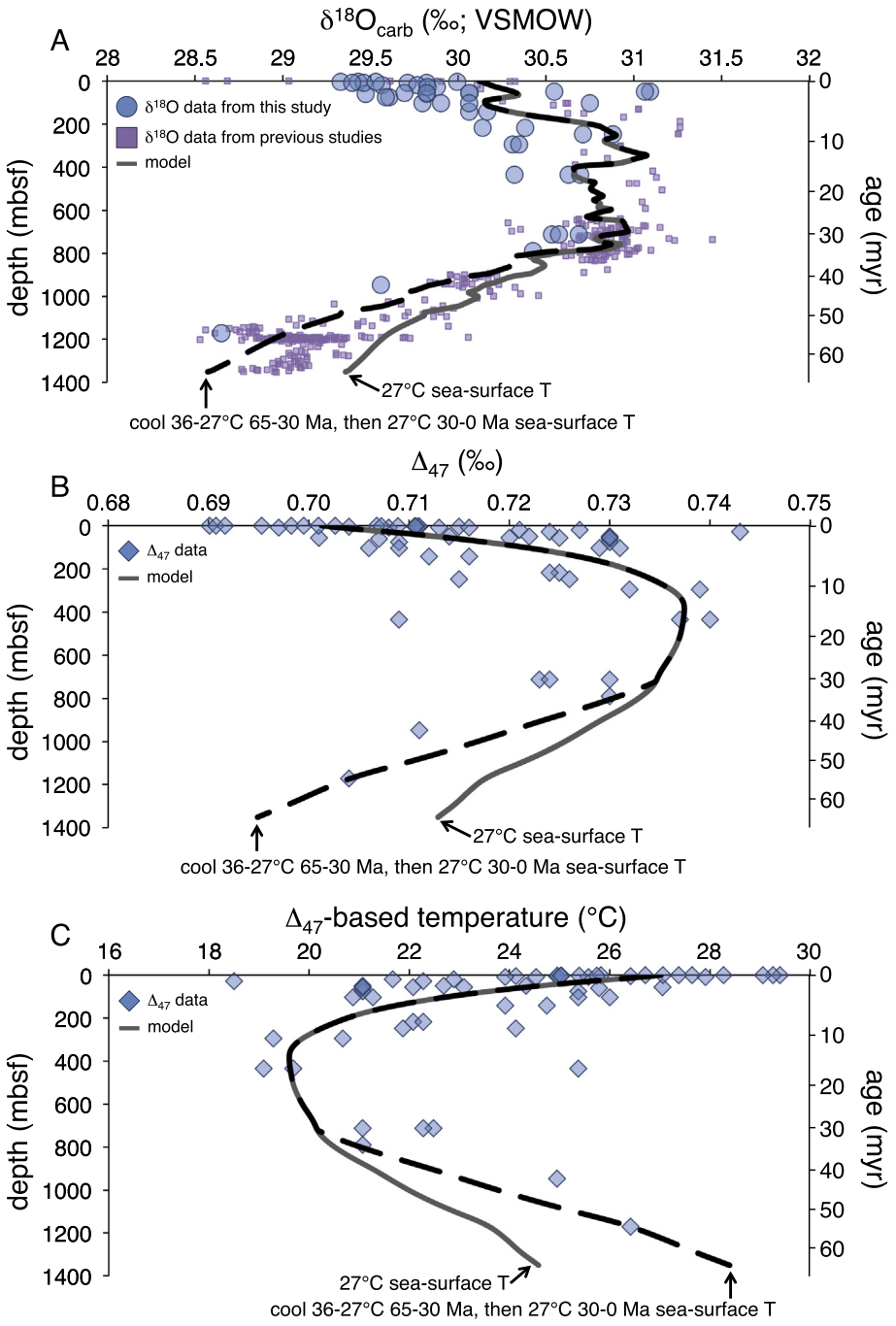

Fig. 9. Comparison of the diagenetic model to site 807 data. Here we have compared a model in which sea-surface temperature is held at 27 °C vs. a model where sea-surface temperatures cools at a constant rate from 36 to 27 °C from 65 to 30 Ma and then remains constant at 27 °C until the present. Cooling over the course of the Paleogene provides a better fit to the data from 60 to 40 Ma.

measurements through the Great Bahama Bank from sites 1003–1007. The temperature data were taken during coring and corrected for thermal effects associated with drilling (Pribnow et al., 2000). These geothermal gradients range from 14 to 37 °C/km, with an average of 29 °C/km. We used 30 °C/km for simplicity. We note that this geotherm is higher than the range given in Winkelstern and Lohmann (2016) of 13–18 °C/km for the area, which is based on unpublished geothermal measurements from the Getty Corporation (Epstein and Clark, 2009). We prefer the ODP-based geothermal gradients as the data and methodology used to calculate them are traceable and were conducted during drilling with the explicit purpose of measuring geothermal gradients (Pribnow et al., 2000).

Finally, we used the 'combined high-temperature' Δ_{47} vs. temperature equation of Defliese et al. (2015), which

was generated in the same laboratory as the clumped-isotope measurements for the Bahamas samples. As discussed in section 2.2, we elected to use the Δ_{47} vs. temperature calibrations generated in the laboratory in which the Δ_{47} measurements were made. We note, though, that this calibration only extends from 5–70 °C. Thus, when diagenesis occurs at temperatures above 70 °C, we had to extrapolate the equation beyond the calibrated temperature range.

For the reaction rate [see Eq. (1)] we used $\beta_{rx} = 6$ (‰/myr), and $\gamma_{rx} = 5$ (myr). These are the same values used in the illustraive deep-sea model (Section 3.1) and shallow-water model (Section 3.2). These are typical values seen in deep-sea settings. As discussed above the value chosen for these parameters is relatively unimportant for the model output as compared to the choice of value for α_{rx}. We ran the model with three different constant background recrystallization rates [α_{rx} — see Eq. (1)] of 0.1, 0.5, and 1 ‰/myr. These values are representative of those used in previous studies of recrystallization in deep-sea settings (Richter and Liang, 1993; Schrag et al., 1995; Schrag, 1999).

Running the model and comparing it to the data demonstrates that background recrystallization rates of 0.5–1‰ per million years show similar trajectories to what is seen in the Bahamas data (Fig. 10). Specifically, Δ_{47} values and Δ_{47}-based temperatures do not change in a measureable way (i.e., beyond 0.01‰) over the first kilometer of burial — as discussed above, this lack of change (despite extensive recrystallization over this depth interval), is due to the similar Δ_{47} values of the carbonate sediment and diagenetic carbonate end members over this depth.

Beginning at about 1 km below the seafloor, noticeable decreases in Δ_{47} values are predicted for background reaction rates of 0.5–1‰/myr (Fig. 10). These changes track the general pattern observed in the data. We note that the geotherm used predicts that for depths below about 3 km, sedimentary temperatures will exceed 100 °C. At this temperature, calcite Δ_{47} values are expected to begin changing on geological timescales due to solid-state isotope-exchange reactions. For example, the model of Stolper and Eiler (2015) predicts that a sample formed at 25 °C and held at 100 °C for 100 million years will experience a Δ_{47}-based temperature increase of 25 °C. Importantly, the most deeply buried samples (below 3.2 km) are dolomite which, empirically, appear not to undergo measureable solid-state reordering reactions in nature until burial temperatures exceed at least ~200 °C (Bonifacie et al., 2013; Lloyd et al., 2017). Thus, the deepest samples (all of which are dolomite) are unlikely to have been affected by solid-state isotope-exchange reactions and we consider it acceptable to model the change in Δ_{47} as solely due to diagenesis. However, future models of deeply buried carbonates should combine the kinetics of diagenetic recrystallization, i.e., dissolution-reprecipitation reactions, and solid-state reordering reactions into a single model framework — but this is beyond the scope of this study. Finally, we note that a geotherm of 15 °C/km, which is the preferred average geotherm of Winkelstern and Lohmann (2016) is also consistent with the diagenetic model, but requires recrystallization rates of about 1 to 1.5 ‰/myr over the 0.5 to 1 ‰/myr for the 30 °C/km geotherm given in Fig. 10.

Ultimately, the model is successful in capturing the first-order trends in the Bahamas dataset both for calcite and dolomite. This indicates that carbonate diagenesis in continental settings can be modeled to first order using the same framework as that previously applied to deep-sea settings and is applicable to both calcite and dolomite. This also suggests that dolomites undergo recrystallization reactions at depth. A key insight from the model is that diagenesis, though it may occur at all stages of burial in shallow-water settings, is unlikely to change Δ_{47} values or Δ_{47}-based temperatures measurably until burial depths exceed ~1 km. This assumes that rates of diagenesis are a monotonic function of sedimentary age. We note that we have not considered massive alteration events due, for example, to the transformation of aragonite to calcite or dolomitization in sediments (Higgins et al., 2018). The model also indicates that elevated Δ_{47} temperatures relative

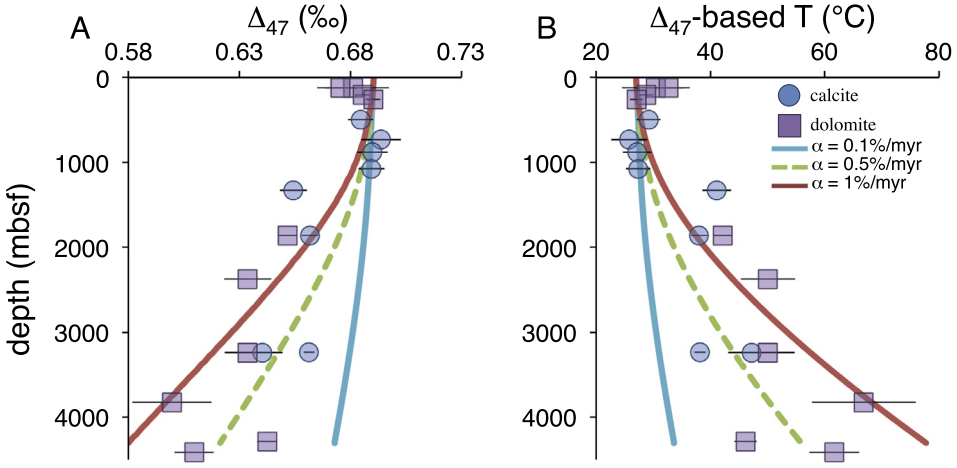

Fig. 10. Comparison of the diagenetic model to data from a drill core through Andros Island, Bahamas. The data is from Winkelstern and Lohmann (2016). Models that use background recrystallization rates (a) of 0.5 to 1 ‰/myr follow the overall trends of the data. See Section 6 for more details of the model. Error bars are 1 s.e.

to formation temperatures that occur due to diagenesis do not necessarily represent a specific recrystallization temperature. Instead, the Δ_{47}-based temperature can be controlled by the contribution of various carbonate phases (both original and diagenetic) that form over a range of temperatures and burial depths (e.g., Stolper and Eiler, 2016).

7. SUMMARY AND CONCLUSIONS

We have presented a model that quantifies the effects of dissolution-reprecipitation reactions on carbonate Δ_{47} values during diagenesis. The model indicates that for systems in which the initial burial temperatures differ substantially (10 s of degrees) from the formation temperatures, noticeable changes in both $\delta^{18}O_{carb}$ and Δ_{47} values occur within the first kilometer of burial. We verified the model using newly presented Δ_{47} values from ODP site 807 in the equatorial Pacific. The model and Δ_{47} data are consistent with previous studies on the effects of diagenesis on $\delta^{18}O_{carb}$ values at this ODP site. This example demonstrates the ability of Δ_{47} values to test and validate models of diagenesis that utilize $\delta^{18}O_{carb}$ values. This is because any model of diagenesis that incorporates changes to $\delta^{18}O_{carb}$ values necessarily predicts the changes in Δ_{47} values. Additionally, the modeling supports previous studies that indicate that equatorial temperatures in the Paleogene western Pacific surface ocean were warmer relative to today.

We additionally explored the model's predictions for shallow-water settings in which formation and the initial diagenesis occur at similar temperatures. Such settings are the dominant sedimentary systems preserved in Mesozoic and older rocks. The model predicts only minor changes in Δ_{47} values (~0.01‰) occur over the first kilometer of burial despite extensive amounts of recrystallization occurring. This is because differences between the temperature of formation and temperature of diagenesis over the first kilometer are generally too small to cause significant changes in Δ_{47} values. However, beyond 1000 mbsf, the influence of diagenesis on Δ_{47} becomes apparent and shifts in Δ_{47} clumped-isotope temperatures of >10 °C are possible depending on the reaction rate. We demonstrated that these insights are consistent with environmental samples by comparing the model to published Δ_{47} data from shallow-water sedimentary carbonates (both calcite and dolomite) from the Bahamas. These data are consistent with the general trend of the model using reaction rates observed in deep-sea settings.

If the model is widely applicable to diagenetic reactions in shallow-water settings, then it indicates that the prevalence of Δ_{47}-based temperatures for ancient samples from 35 to 50 °C may be due, at least in part, to the continual incorporation of diagenetic carbonates formed during diagenesis at all stages of burial. This conclusion is consistent with the interpretation and quantitative modeling of phosphorite diagenesis based on clumped-isotope measurements (Stolper and Eiler, 2016). This interpretation of elevated Δ_{47}-based temperatures is different from some interpretations of Δ_{47}-based temperatures of diagenetically modified carbonates as the singular temperature of reequilibration. In such interpretations, the Δ_{47}-based temperatures are taken to indicate the mean temperature of diagenesis and are used in conjunction with $\delta^{18}O_{carb}$ values to calculate $\delta^{18}O_{fluid}$ values of ancient pore fluids. Instead, the model presented here indicates that Δ_{47}-based temperatures of diagenetically altered carbonates are the result of the precipitation and dissolution of carbonate at all stages of burial and do not represent any single diagenetic event.

It is important to note here that the model may only be appropriate for fine grained sediments as occurs today in deep-sea sediments formed from foraminifera and coccolithophores and platform carbonates dominantly derived from the precipitation of small carbonate particles in the water column (as in the Bahamas). The rates of diagenesis of buried macroscale invertebrate (or vertebrate) fossils (e.g., corals, brachiopods, etc) could vary as a function of the fossil material and differ from fine-grained carbonates. A potential future area of research would be to study differences in recrystallization rates in different fossils vs. micrite cements from a core or outcrop of a carbonate system in order to constrain how such diagenetic rates may differ. Regardless, the model presented here provides the framework for evaluating the effects of diagenesis on Δ_{47} values and, potentially, to correct for them. Finally, a potential next step is to make a unified model of diagenesis and solid-state isotope-exchange reactions so that the effects of each can be understood together in the context of a sample's burial history.

ACKNOWLEDGEMENTS

DAS acknowledges support from the NSF GRFP and NOAA Climate and Global Change Postdoctoral fellowship. JAH acknowledges the ODP program for providing samples. We thank Hagit Affek, D. Schrag and two anonymous reviewers for constructive comments.

APPENDIX A

A.1. ^{17}O corrections

Schauer et al. (2016) and Daëron et al. (2016) recently showed that Δ_{47} values can vary subtly as a function of a sample's $\delta^{13}C$ and $\delta^{18}O$ values based on the choice of the isotopic compositions (i.e., $^{18}O/^{16}O$, $^{17}O/^{16}O$ and $^{13}C/^{12}C$ values) for VSMOW and VPDB. We used the values for these standards given in Santrock et al. (1985). Schauer et al. (2016) and Daëron et al. (2016) showed that the use of the Santrock et al. (1985) values can create a dependence of measured Δ_{47} values on a sample's $\delta^{13}C$ and $\delta^{18}O$ values. This dependence is apparent when sample $\delta^{13}C$ values vary by 10 s of per mil. We used the Santrock et al. (1985) values here for the following reasons: (*i*) all previous Δ_{47} measurements made at Caltech, including calibrations to convert Δ_{47} values to formation temperatures, were made using the isotopic compositions of VSMOW and VDPB given in Santrock et al. (1985). (*ii*) Samples measured here vary by at most 3.5‰ in $\delta^{13}C$ from each other and 6.8‰ from the reference gas. Based on observations from Schauer et al. (2016), this difference in $\delta^{13}C$ could induce Δ_{47} inaccuracies of at most 0.008‰ between samples using the

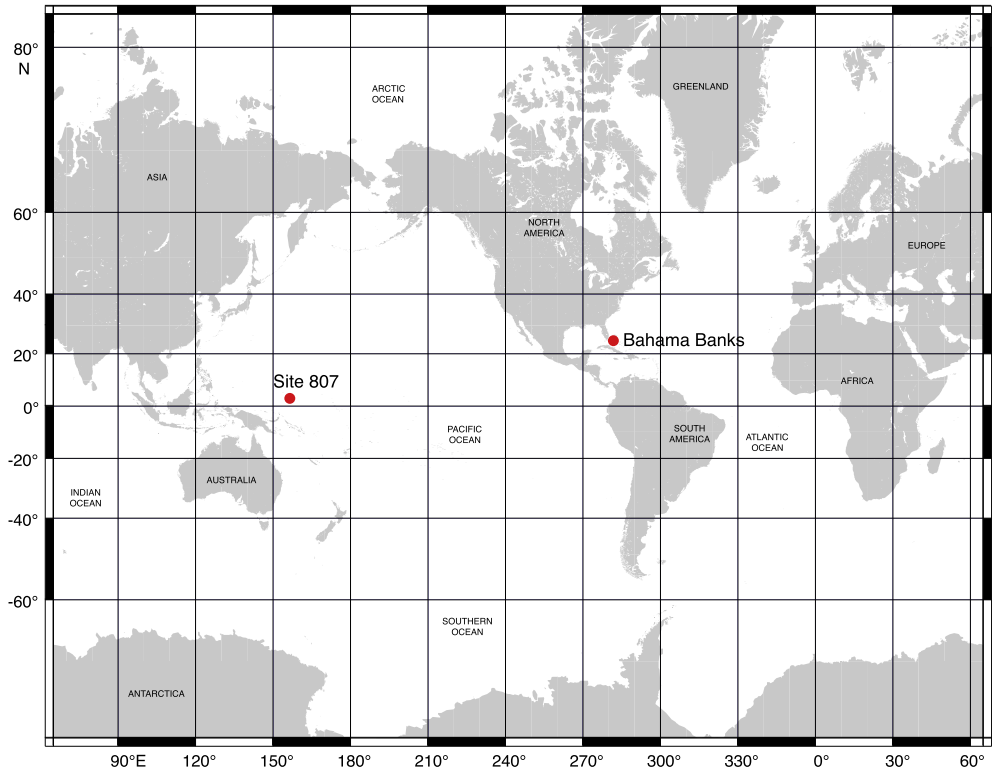

Fig. A1. Location of Ocean Drilling Project site 807 as well as the Bahama Banks drill site discussed in Winkelstern and Lohmann (2016). Map modified from Wessel et al. (2013).

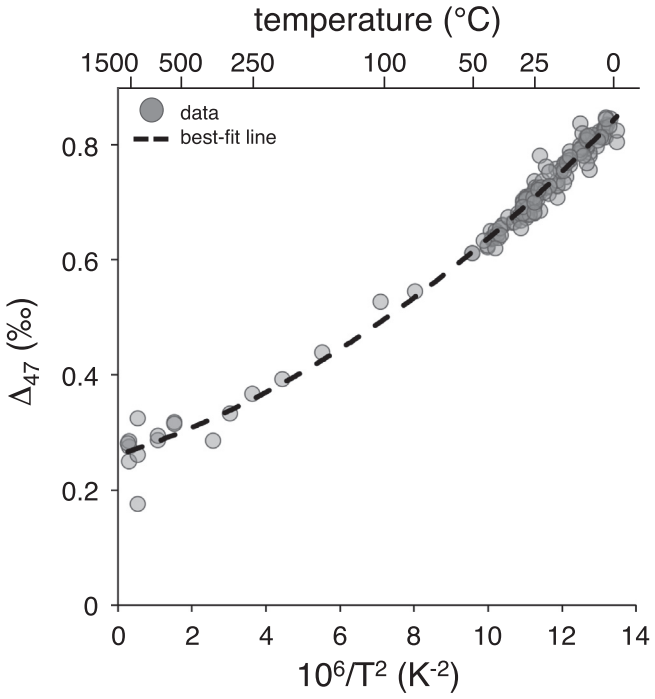

Fig. A2. Δ_{47} vs. temperature calibration used to simulate diagenesis at temperatures beyond 50 °C, which is the highest temperature used in the Ghosh et al. (2006) calibration. This calibration was used solely in the model output presented in Fig. 10. The equation is $\Delta_{47} = 0.00173 \times (10^6/T^2)^2 + 0.0203 \times 10^6/T^2 + 0.261$ where T is the temperature in Kelvin. Data used in this calibration comes only from measurements made at the Caltech laboratories (Ghosh et al., 2006, 2007; Came et al., 2007; Guo et al., 2009; Tripati et al., 2010; Eagle et al., 2010, 2015; Thiagarajan et al., 2011; Dennis et al., 2011; Stolper and Eiler, 2015; Spooner et al., 2016; Bonifacie et al., 2017).

Santrock et al. (1985) values. We consider such differences negligible for our purposes given that typical Δ_{47} standard errors range ±0.01–0.02‰ (*iii*) Foraminifera from the Ontong Java Plateau measured in the Caltech laboratory using the same methodology as employed here (including a 90 °C acid bath) and the Santrock et al. (1985) standard values, yielded clumped isotope temperatures of 28.5 °C ± 0.2 (1σ) and within 2σ error of the local temperature 29.2 °C ± 0.4 (Tripati et al., 2010, 2014). Tripati et al. (2010) also demonstrated that Δ_{47} values of deep-sea carbonates conform to the Δ_{47} vs. temperature calibration of Ghosh et al. (2006). Additionally, Daëron et al. (2016) demonstrated that choice of $^{18}O/^{16}O$, $^{17}O/^{16}O$ and $^{13}C/^{12}C$ for VSMOW and VPDB does not appear to affect the temperature dependence (i.e., the slope) of Δ_{47} vs. $1/T^2$ calibrations. Because the Ghosh et al. (2006) calibration yields accurate Δ_{47}-based temperatures for modern samples in our study area with known formations temperatures and the temperature dependence of Δ_{47} vs. $1/T^2$ calibrations is apparently independent of the choice of VSMOW and VPDB values, we consider our use of the Santrock et al. (1985) value to be appropriate for this study.

A.2: Δ_{47} values and end-member mixing

Here we further justify our assumption that we can treat Δ_{47} values of mixtures of multiple carbonate components as the weighted averaged (by weight percent) of the Δ_{47} value of the end members. This assumption is valid when the $\delta^{13}C$ and $\delta^{18}O$ values of the end members do not differ sufficiently to induce significant non-linear mixing effects (Eiler and Schauble, 2004; Defliese and Lohmann, 2015).

The isotopic composition of the diagenetic and sedimentary carbonate components can differ due to temperature-dependent equilibrium isotope effects. For example, carbonate isotopically equilibrated with water at 50 °C is

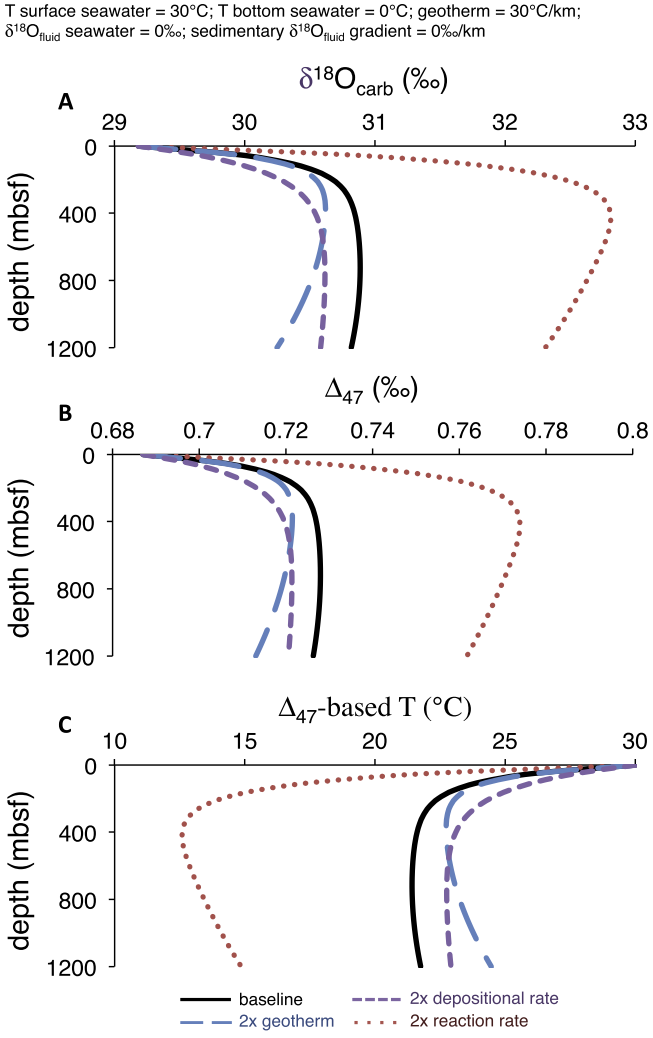

Fig. A3. Comparison of changes in various model parameters including the geothermal gradient, depositional rate, and reaction rate on the effects of diagenesis on $\delta^{18}O$, Δ_{47} values, and Δ_{47}-based temperatures. The baseline model is the same as that given in Fig. 2 (see Section 3.1.4). When reaction rates are doubled (red line), we double α_{rx}, β_{rx}, and γ_{rx}.

~11‰ lower in $\delta^{18}O$ than carbonate equilibrated with the same water at −2° (Kim and O'Neil, 1997; Watkins et al., 2013). −2 °C represents the approximate minimum water temperatures seen in the oceans today while 50 °C is a typical temperature 1 km below the seafloor. In contrast, the difference between carbonate vs. dissolved inorganic carbonate $\delta^{13}C$ values of experimentally precipitated carbonates from 10 to 40 °C (the total experimental range) shows no dependence on temperature (Romanek et al., 1992; Zeebe and Wolf-Gladrow, 2001). Based on this, mixing of carbonates formed in isotopic equilibrium with pore fluids (both carbon and oxygen isotope equilibrium) at −2 and 50 °C generates a maximum mixing nonlinearity for Δ_{47} of 0.0005‰ relative to assuming Δ_{47} values mix linearly as a function of the weight percent of each component. This non-linearity is significantly less than the precision of typical Δ_{47} measurements (~±0.01‰ 1σ) and thus can be ignored.

The above calculation assumes that the dissolved inorganic carbon in the fluid is in equilibrium with the carbonate at a given depth and that the two are identical. This assumption can fail if significant amounts of organic carbon, which is lower in $\delta^{13}C$ than marine carbonates (typically by ~25‰ over the past 200 million years; e.g., Falkowski et al., 2005) is incorporated into the dissolved inorganic carbon pool and then precipitated as diagenetic carbonate. Importantly, at site 807, typical organic carbon weight percents (by dry weight) are <0.1% (Stax and Stein, 1993) compared to >90% for carbonate (Kroenke et al., 1991). Thus, as there are orders of magnitude more carbon in carbonates that in organic carbon in this system, we consider it acceptable to ignore the influence of respiration on the dissolved inorganic pool. Additionally, as discussed in Section 4.3 and in Fig. 5, changes in site 807 $\delta^{13}C_{carb}$ with time mirror changes in global records of carbonates over the Cenozoic (Zachos et al., 2001). This further supports our argument that $\delta^{13}C$ values of diagenetic carbonates are similar to the bulk sediment being dissolved.

A.3. Details on recrystallization rates

In our modeling of site 807 data above, we used the recrystallization rates given by Schrag et al. (1995) for site 807. Fantle and DePaolo (2006) provide different and lower recrystallization rates for site 807 based on carbonate and pore fluid Sr concentrations and isotopic compositions from 0 to 800 mbsf. Their model has no background recrystallization rate such that $\alpha_{rx} = 0$ %/myr vs. 0.5 %/myr in Schrag et al. (1995). They did invoke an exponential decaying reaction rate with time with a maximum recrystallization rate (β_{rx}; 3.5 %/myr) half that given in Schrag et al. (1995), though with a longer e-folding time (γ_{rx}) of 11 myr vs. 9 myr in Schrag et al. (1995). Over the first 1000 km, this leads to 2x less recrystallization (40%) than the model of Schrag et al. (1995; 90%). In a follow-up study by the same authors (Fantle and DePaolo, 2007), the age-dependent recrystallization rate of Fantle and DePaolo (2006) (the β_{rx} term), was determined to be too low for sediments less than 2.5 million years old (<50 mbsf). This determination was based on modeling of calcium concen-

Table A1
$\delta^{13}C$ and $\delta^{18}O$ accuracy and precision of standards and site 807 samples.

	n[a]	Uncorrected[b] $\delta^{18}O_{this\ study}$ (‰)[c]	1σ[d] uncorrected	Corrected[e] $\delta^{18}O_{this\ study}$ (‰)[c]	1σ[d] corrected	$\delta^{18}O_{Caltech}$ (‰)[c,f]	Uncorrected[b] $\delta^{13}C_{this\ study}$ (‰)[g]	1σ[d] uncorrected	Corrected[e] $\delta^{13}C_{this\ study}$ (‰)[g]	1σ[d] corrected	$\delta^{13}C_{Caltech}$ (‰)[f,g]
Carrara marble	43	28.72	0.28	28.84	0.07	28.83	2.29	0.11	2.32	0.04	2.33
TV01	41	21.95	0.2	22.02	0.05	22.03	2.50	0.11	2.53	0.05	2.53
Site 807 averages[h]	116	–	0.16	–	0.06	–	–	0.09	–	0.07	–

[a] Number of samples measured.
[b] Measured values before correction based on differences between values of standards in an analytical session vs. the long-term average.
[c] Referenced to VSMOW.
[d] 1 standard deviation.
[e] Measured values after correction based on differences between values of standards in an analytical session vs. the long-term average.
[f] Average, long-term value at Caltech.
[g] Referenced to the VPDB scale.
[h] Only the pooled standard deviation for the precision of all site 807 measurements is given. No average is given as all site 807 samples are used for this analysis.

Table A2
Δ_{47} accuracy and precision of standards and site 807 samples.

	n[a]	$\Delta_{47,\ \text{this study}}$ (‰)[b]	1σ[c]	$\Delta_{47,\ \text{Caltech}}$ (‰)[b,d]	Δ_{47}, Dennis et al. (2011) (‰)[b,e]
Carrara Marble	43	0.409	0.011	0.401	0.403
TV01	41	0.729	0.016	0.724	–
site 807 averages[f]	116	–	0.012	–	–

[a] Number of samples measured.
[b] Given in the absolute reference frame (ARF) of Dennis et al. (2011).
[c] 1 standard deviation.
[d] Average, long-term value at Caltech.
[e] This value (in the absolute reference frame) is derived from Dennis et al. (2011) by taking the average value for the reported Carrara in-house marbles and increasing the Harvard, Johns Hopkins, and Caltech values by 0.011‰ to account for the 90 °C clumped-isotope acid-digestion fractionation factor value of 0.092‰ used in this study instead of 0.081‰ as was used in that study.
[f] Only the pooled standard deviation for the precision of all site 807 measurements is given. No average is given as all site 807 samples are used for this analysis.

trations and isotopic compositions of pore fluids and solids. Fantle and DePaolo (2007) suggested initial recrystallization rates are 30–40%/myr over this depth range (top 50 m), increasing total recrystallization over the first kilometer of burial up to ~60%.

The remaining difference in total recrystallization rate between the two studies occurs because Fantle and DePaolo (2006) chose α_{rx} to be 0 %/myr while Schrag et al. (1995) chose α_{rx} to be 0.5 %/myr. Significant recrystallization of sediments at depth is evidenced by the physical properties and petrography of sediments below 500 mbsf. Specifically, chalk begins to convert to limestone beginning at ~850 mbsf (Borre and Fabricius, 1998). Chalk is distinguished from limestone based on how easy it is to mechanically deform. Specifically, chalk can be deformed with a metal spatula while limestone is hard enough that a saw is required to cut it (Schlanger et al., 1973). This difference in material properties is the result of the presence of carbonate cements in limestone that bind grains together via the filling and loss of porosity. These cements are chemical precipitates and necessitate the contribution of carbonate formed in the sediments to the solid phase. The importance of the chalk-limestone transition for measured recrystallization rates was noted by Higgins and Schrag (2012) for site 807. They required extensive (6 %/myr) recrystallization to occur during the conversion of chalk to limestone at depths from 1100–1300 m in order to fit carbonate and pore-fluid magnesium concentrations and isotopic compositions. Fantle and DePaolo (2006) did not need to consider this as they focused on diagenesis only from 0 to 800 mbsf.

We chose to use the recrystallization rates of Schrag et al. (1995) as these capture the extensive recrystallization in the top few hundred meters of the sediment column, consistent with the findings of Fantle and DePaolo (2007), and capture the extensive recrystallization at depths below 800 mbsf during the chalk-limestone transition.

APPENDIX B. SUPPLEMENTARY MATERIAL

Supplementary data associated with this article can be found, in the online version, at https://doi.org/10.1016/j.gca.2018.01.037.

REFERENCES

Adkins J. F., McIntyre K. and Schrag D. P. (2002) The salinity, temperature, and $\delta^{18}O$ of the glacial deep ocean. *Science* **298**, 1769–1773.

Affek H. P. and Eiler J. M. (2006) Abundance of mass 47 CO_2 in urban air, car exhaust, and human breath. *Geochim. Cosmochim. Acta* **70**, 1–12.

Banner J. L. and Hanson G. N. (1990) Calculation of simultaneous isotopic and trace element variations during water-rock interaction with applications to carbonate diagenesis. *Geochim. Cosmochim. Acta* **54**, 3123–3137.

Bergmann K. D., Finnegan S., Creel R., Eiler J. M., Hughes N. C., Popov L. E. and Fischer W. W. (2018) A paired apatite and calcite clumped isotope thermometry approach to estimating Cambro-Ordovician seawater temperatures and isotopic composition. *Geochim. Cosmochim. Acta* **224**, 18–41.

Bernard S., Daval D., Ackerer P., Pont S. and Meibom A. (2017) Burial-induced oxygen-isotope re-equilibration of fossil foraminifera explains ocean paleotemperature paradoxes. *Nat. Commun.* **8**, 1134.

Bijl P. K., Schouten S., Sluijs A., Reichart G.-J., Zachos J. C. and Brinkhuis H. (2009) Early Palaeogene temperature evolution of the southwest Pacific Ocean. *Nature* **461**, 776–779.

Bonifacie M., Calmels D. and Eiler J. (2013) Clumped isotope thermometry of marbles as an indicator of the closure temperatures of calcite and dolomite with respect to solid-state reordering of C–O bonds. *Mineral Mag.* **77**, 735.

Bonifacie M., Calmels D., Eiler J. M., Horita J., Chaduteau C., Vasconcelos C., Agrinier P., Katz A., Passey B. H. and Ferry J. M. (2017) Calibration of the dolomite clumped isotope thermometer from 25 to 350 C, and implications for a universal calibration for all (Ca, Mg, Fe) CO_3 carbonates. *Geochim. Cosmochim. Acta* **200**, 255–279.

Borre M. and Fabricius I. L. (1998) Chemical and mechanical processes during burial diagenesis of chalk: an interpretation based on specific surface data of deep-sea sediments. *Sedimentology* **45**, 755–769.

Brand U. and Veizer J. (1981) Chemical diagenesis of a multicomponent carbonate system-2: stable isotopes. *J. Sediment. Res.* **51**.

Came R. E., Brand U. and Affek H. P. (2014) Clumped isotope signatures in modern brachiopod carbonate. *Chem. Geol.* **377**, 20–30.

Came R. E., Eiler J. M., Veizer J., Azmy K., Brand U. and Weidman C. R. (2007) Coupling of surface temperatures and

atmospheric CO_2 concentrations during the Palaeozoic era. *Nature* **449**, 198–201.

Chandler M. T., Wessel P., Taylor B., Seton M., Kim S.-S. and Hyeong K. (2012) Reconstructing Ontong Java Nui: Implications for Pacific absolute plate motion, hotspot drift and true polar wander. *Earth Planet Sci. Lett.* **331**, 140–151.

Coplen T. B., Brand W. A., Gehre M., Gröning M., Meijer H. A., Toman B. and Verkouteren R. M. (2006) New guidelines for $\delta^{13}C$ measurements. *Anal. Chem.* **78**, 2439–2441.

Corfield R. M. and Cartlidge J. E. (1993) Whole-rock oxygen and carbon isotope stratigraphy of the Paleogene and Cretaceous/Tertiary boundary in Hole 807C. *Proc. ODP Sci. Results* **130**, 259–268.

Craig H. and Gordon L. I. (1965) Deuterium and oxygen 18 variations in the ocean and the marine atmosphere. In *Stable Isotopes in Oceanographic Studies and Paleotemperatures* (ed. E. Tongiorgi), pp. 9–130.

Cramer B., Miller K., Barrett P. and Wright J. (2011) Late Cretaceous-Neogene trends in deep ocean temperature and continental ice volume: reconciling records of benthic foraminiferal geochemistry (δ18O and Mg/Ca) with sea level history. *J. Geophys. Res. Oceans* **116**.

Criss R. E. (1999) *Principles of Stable Isotope Distribution*. Oxford University Press, New York.

Daeron M., Blamart D., Drysdale R., Coplen T. and Zanchetta G. (2017) Can we learn anything new from yet another carbonate calibration? In *6th International Clumped Isotope Workshop, Paris, France*.

Daëron M., Blamart D., Peral M. and Affek H. (2016) Absolute isotopic abundance ratios and the accuracy of Δ_{47} measurements. *Chem. Geol.* **442**, 83–96.

de Garidel-Thoron T., Rosenthal Y., Bassinot F. and Beaufort L. (2005) Stable sea surface temperatures in the western Pacific warm pool over the past 1.75 million years. *Nature* **433**, 294.

Defliese W. F., Hren M. T. and Lohmann K. C. (2015) Compositional and temperature effects of phosphoric acid fractionation on Δ_{47} analysis and implications for discrepant calibrations. *Chem. Geol.*.

Defliese W. F. and Lohmann K. C. (2015) Non-linear mixing effects on mass-47 CO_2 clumped isotope thermometry: patterns and implications. *Rapid. Commun. Mass Spectrom.* **29**, 901–909.

Dennis K. J., Affek H. P., Passey B. H., Schrag D. P. and Eiler J. M. (2011) Defining an absolute reference frame for 'clumped' isotope studies of CO_2. *Geochim. Cosmochim. Acta* **75**, 7117–7131.

Dennis K. J. and Schrag D. P. (2010) Clumped isotope thermometry of carbonatites as an indicator of diagenetic alteration. *Geochim. Cosmochim. Acta* **74**, 4110–4122.

Dietzel M., Tang J., Leis A. and Köhler S. J. (2009) Oxygen isotopic fractionation during inorganic calcite precipitation – effects of temperature, precipitation rate and pH. *Chem. Geol.* **268**, 107–115.

Douglas P. M., Affek H. P., Ivany L. C., Houben A. J., Sijp W. P., Sluijs A., Schouten S. and Pagani M. (2014) Pronounced zonal heterogeneity in Eocene southern high-latitude sea surface temperatures. *Proc. Natl. Acad. Sci.* **111**, 6582–6587.

Dyer B., Higgins J. A. and Maloof A. C. (2017) A probabilistic analysis of meteorically altered $\delta^{13}C$ chemostratigraphy from late Paleozoic ice age carbonate platforms. *Geology* **45**, 135–138.

Eagle R. A., Enriquez M., Grellet-Tinner G., Pérez-Huerta A., Hu D., Tütken T., Montanari S., Loyd S. J., Ramirez P. and Tripati A. K. (2015) Isotopic ordering in eggshells reflects body temperatures and suggests differing thermophysiology in two Cretaceous dinosaurs. *Nat. Commun.* **6** (Art. No. 82960.

Eagle R. A., Schauble E. A., Tripati A. K., Tütken T., Hulbert R. C. and Eiler J. M. (2010) Body temperatures of modern and extinct vertebrates from ^{13}C–^{18}O bond abundances in bioapatite. *Proc. Natl. Acad. Sci.* **107**, 10377.

Eiler J. M. (2011) Paleoclimate reconstruction using carbonate clumped isotope thermometry. *Quat. Sci. Rev.* **30**, 3575–3588.

Eiler J. M. and Schauble E. (2004) $^{18}O^{13}C^{16}O$ in Earth's atmosphere. *Geochim. Cosmochim. Acta* **68**, 4767–4777.

Elderfield H., Gieskes J. M., Baker P. A., Oldfield R., Hawkesworth C. and Miller R. (1982) $^{87}Sr/^{86}Sr$ and $^{18}O/^{16}O$ ratios, interstitial water chemistry and diagenesis in deep-sea carbonate sediments of the Ontong Java Plateau. *Geochim. Cosmochim. Acta* **46**, 2259–2268.

Emiliani C. (1955) Pleistocene temperatures. *J. Geol.*, 538–578.

Epstein S. A. and Clark D. (2009) Hydrocarbon potential of the Mesozoic carbonates of the Bahamas. *Carbonates Evaporites* **24**, 97–138.

Erez J. (1978) Vital effect on stable-isotope composition seen in foraminifera and coral skeletons. *Nature* **273**, 199–202.

Falkowski P. G., Katz M. E., Milligan A. J., Fennel K., Cramer B. S., Aubry M. P., Berner R. A., Novacek M. J. and Zapol W. M. (2005) The rise of oxygen over the past 205 million years and the evolution of large placental mammals. *Science* **309**, 2202–2204.

Fantle M., Maher K. and DePaolo D. (2010) Isotopic approaches for quantifying the rates of marine burial diagenesis. *Rev. Geophys.* **48**.

Fantle M. S. (2015) Calcium isotopic evidence for rapid recrystallization of bulk marine carbonates and implications for geochemical proxies. *Geochim. Cosmochim. Acta* **148**, 378–401.

Fantle M. S. and DePaolo D. J. (2006) Sr isotopes and pore fluid chemistry in carbonate sediment of the Ontong Java Plateau: calcite recrystallization rates and evidence for a rapid rise in seawater Mg over the last 10 million years. *Geochim. Cosmochim. Acta* **70**, 3883–3904.

Fantle M. S. and DePaolo D. J. (2007) Ca isotopes in carbonate sediment and pore fluid from ODP Site 807A: the Ca^{2+}(aq)–calcite equilibrium fractionation factor and calcite recrystallization rates in Pleistocene sediments. *Geochim. Cosmochim. Acta* **71**, 2524–2546.

Finnegan S., Bergmann K., Eiler J. M., Jones D. S., Fike D. A., Eisenman I., Hughes N. C., Tripati A. K. and Fischer W. W. (2011) The magnitude and duration of Late Ordovician-Early Silurian glaciation. *Science* **331**, 903.

Ghosh P., Adkins J., Affek H., Balta B., Guo W., Schauble E. A., Schrag D. and Eiler J. M. (2006) ^{13}C–^{18}O bonds in carbonate minerals: a new kind of paleothermometer. *Geochim. Cosmochim. Acta* **70**, 1439–1456.

Ghosh P., Eiler J., Campana S. E. and Feeney R. F. (2007) Calibration of the carbonate 'clumped isotope' paleothermometer for otoliths. *Geochim. Cosmochim. Acta* **71**, 2736–2744.

Grauel A.-L., Schmid T. W., Hu B., Bergami C., Capotondi L., Zhou L. and Bernasconi S. M. (2013) Calibration and application of the 'clumped isotope' thermometer to foraminifera for high-resolution climate reconstructions. *Geochim. Cosmochim. Acta* **108**, 125–140.

Gregory R. (1991) Oxygen isotope history of seawater revisited: timescales for boundary event changes in the oxygen isotope composition of seawater. In *Stable Isotope Geochemistry: A Tribute to Samuel Epstein*, pp. 65–76. Stable Isotope Geochemistry: A Tribute to Samuel Epstein. The Geochemical Society, San Antonio, USA.

Gregory R. T. and Taylor H. P. (1981) An oxygen isotope profile in a section of Cretaceous oceanic crust, Samail Ophiolite, Oman: Evidence for $\delta^{18}O$ buffering of the oceans by deep (>5 km)

seawater-hydrothermal circulation at mid-ocean ridges. *J. Geophys. Res. Solid Earth* **86**, 2737–2755.

Guo W., Mosenfelder J. L., Goddard, III, W. A. and Eiler J. M. (2009) Isotopic fractionations associated with phosphoric acid digestion of carbonate minerals: insights from first-principles theoretical modeling and clumped isotope measurements. *Geochim. Cosmochim. Acta* **73**, 7203–7225.

Henkes G. A., Passey B. H., Grossman E. L., Shenton B. J., Pérez-Huerta A. and Yancey T. E. (2014) Temperature limits for preservation of primary calcite clumped isotope paleotemperatures. *Geochim. Cosmochim. Acta* **139**, 362–382.

Henkes G. A., Passey B. H., Wanamaker A. D., Grossman E. L., Ambrose W. G. and Carroll M. L. (2013) Carbonate clumped isotope compositions of modern marine mollusk and brachiopod shells. *Geochim. Cosmochim. Acta*.

Higgins J., Blättler C., Lundstrom E., Santiago-Ramos D., Akhtar A., Ahm A. C., Bialik O., Holmden C., Bradbury H. and Murray S. (2018) Mineralogy, early marine diagenesis, and the chemistry of shallow-water carbonate sediments. *Geochim. Cosmochim. Acta* **220**, 512–534.

Higgins J. and Schrag D. (2012) Records of Neogene seawater chemistry and diagenesis in deep-sea carbonate sediments and pore fluids. *Earth Planet. Sci. Lett.* **357**, 386–396.

Huntington K., Eiler J., Affek H., Guo W., Bonifacie M., Yeung L., Thiagarajan N., Passey B., Tripati A. and Daëron M. (2009) Methods and limitations of 'clumped' CO_2 isotope (Δ_{47}) analysis by gas-source isotope ratio mass spectrometry. *J. Mass Spectrom.* **44**, 1318–1329.

Jaffrés J. B. D., Shields G. A. and Wallmann K. (2007) The oxygen isotope evolution of seawater: a critical review of a long-standing controversy and an improved geological water cycle model for the past 3.4 billion years. *Earth Sci. Rev.* **83**, 83–122.

Kasting J. F., Howard M. T., Wallmann K., Veizer J., Shields G. and Jaffrés J. (2006) Paleoclimates, ocean depth, and the oxygen isotopic composition of seawater. *Earth Planet. Sci. Lett.* **252**, 82–93.

Katz A., Bonifacie M., Hermoso M., Cartigny P. and Calmels D. (2017) Laboratory-grown coccoliths exhibit no vital effect in clumped isotope (Δ_{47}) composition on a range of geologically relevant temperatures. *Geochim. Cosmochim. Acta* **208**, 335–353.

Kele S., Breitenbach S. F., Capezzuoli E., Meckler A. N., Ziegler M., Millan I. M., Kluge T., Deák J., Hanselmann K. and John C. M. (2015) Temperature dependence of oxygen-and clumped isotope fractionation in carbonates: a study of travertines and tufas in the 6–95 C temperature range. *Geochim. Cosmochim. Acta* **168**, 172–192.

Kelson J. R., Huntington K. W., Schauer A. J., Saenger C. and Lechler A. R. (2017) Toward a universal carbonate clumped isotope calibration: diverse synthesis and preparatory methods suggest a single temperature relationship. *Geochim. Cosmochim. Acta* **197**, 104–131.

Killingley J. S. (1983) Effects of diagenetic recrystallization on $^{18}O/^{16}O$ values of deep-sea sediments. *Nature* **301**, 594–597.

Kim S. T. and O'Neil J. R. (1997) Equilibrium and nonequilibrium oxygen isotope effects in synthetic carbonates. *Geochim. Cosmochim. Acta* **61**, 3461–3475.

Kluge T., John C. M., Jourdan A.-L., Davis S. and Crawshaw J. (2015) Laboratory calibration of the calcium carbonate clumped isotope thermometer in the 25–250 C temperature range. *Geochim. Cosmochim. Acta* **157**, 213–227.

Kozdon R., Kelly D. C., Kita N. T., Fournelle J. H. and Valley J. W. (2011) Planktonic foraminiferal oxygen isotope analysis by ion microprobe technique suggests warm tropical sea surface temperatures during the Early Paleogene. *Paleoceanography* **26**.

Kramer P. A., Swart P. K., De Carlo E. H. and Schovsbo N. H. (2000) Overview of interstitial fluid and sediment geochemistry, sites 1003–1007 (Bahamas transect). *Proc. ODP Sci. Results* **166**, 179–195.

Kroenke L., Berger W. and Janecek T. (1991) Site 807. *Proc. ODP Initial Rep.*, 369–493.

Kroopnick P. (1985) The distribution of ^{13}C of ΣCO_2 in the world oceans. *Deep Sea Res. Part A: Oceanogr. Res. Pap.* **32**, 57–84.

Lawrence J. and Gieskes J. (1981) Constraints on water transport and alteration in the oceanic crust from the isotopic composition of pore water. *J. Geophys. Res. Solid Earth* **86**, 7924–7934.

Lear C. H., Elderfield H. and Wilson P. (2000) Cenozoic deep-sea temperatures and global ice volumes from Mg/Ca in benthic foraminiferal calcite. *Science* **287**, 269–272.

LeGrande A. N. and Schmidt G. A. (2006) Global gridded data set of the oxygen isotopic composition in seawater. *Geophys. Res. Lett.* **33**.

Lloyd M. K., Eiler J. M. and Nabelek P. I. (2017) Clumped isotope thermometry of calcite and dolomite in a contact metamorphic environment. *Geochim. Cosmochim. Acta* **197**, 323–344.

Locarnini R., Mishonov A., Antonov J., Boyer T. and Garcia H. (2006) World Ocean Atlas 2005, Volume 1: Temperature. In *NOAA Atlas NESDIS 61* (ed. S. Levitus). U.S. Government Printing Office, Washington, D.C., p. 182.

McCrea J. M. (1950) On the isotopic chemistry of carbonates and a paleotemperature scale. *J. Chem. Phys.* **18**, 849–857.

Melim L., Westphal H., Swart P. K., Eberli G. P. and Munnecke A. (2002) Questioning carbonate diagenetic paradigms: evidence from the Neogene of the Bahamas. *Mar. Geol.* **185**, 27–53.

Melim L. A., Swart P. K. and Maliva R. G. (2001) Meteoric and marine-burial diagenesis in the subsurface of Great Bahama Bank. *Spec. Publ.-SEPM* **70**, 137–162.

Miller K. G., Fairbanks R. G. and Mountain G. S. (1987) Tertiary oxygen isotope synthesis, sea level history, and continental margin erosion. *Paleoceanography* **2**, 1–19.

Muehlenbachs K. and Clayton R. (1976) Oxygen isotope composition of the oceanic crust and its bearing on seawater. *J. Geophys. Res.* **81**, 4365–4369.

Passey B. and Henkes G. (2012) Carbonate clumped isotope bond reordering and geospeedometry. *Earth Planet. Sci. Lett.* **351–352**, 223–236.

Passey B. H., Levin N. E., Cerling T. E., Brown F. H. and Eiler J. M. (2010) High-temperature environments of human evolution in East Africa based on bond ordering in paleosol carbonates. *Proc. Natl. Acad. Sci.* **107**, 11245.

Pearson P. N., Ditchfield P. W., Singano J., Harcourt-Brown K. G., Nicholas C. J., Olsson R. K., Shackleton N. J. and Hall M. A. (2001) Warm tropical sea surface temperatures in the Late Cretaceous and Eocene epochs. *Nature* **413**, 481–487.

Petersen S. and Schrag D. (2015) Antarctic ice growth before and after the Eocene-Oligocene transition: new estimates from clumped isotope paleothermometry. *Paleoceanography* **30**, 1305–1317.

Prentice M., Friez J., Simonds G. and Matthews R. (1993) Neogene trends in planktonic foraminifer $\delta^{18}O$ from Site 807: Implications for global ice volume and western equatorial Pacific sea-surface temperatures. In *Proceedings of the Ocean Drilling Program, Scientific Results*, 130 (eds. W. H. Berger, L. A. Kroenke and L. A. Mayer), pp. 281–305.

Pribnow D. F. C., Kinoshita M. and Stein C. A. (2000) *Thermal Data Collection and Heat Flow Recalculations for ODP Legs 101–180*. Institute for Joint Geoscientific Research, GGA, Hanover, Germany, p. 0120432.

Richter F. M. and DePaolo D. J. (1987) Numerical models for diagenesis and the Neogene Sr isotopic evolution of seawater from DSDP Site 590B. *Earth Planet. Sci. Lett.* **83**, 27–38.

Richter F. M. and DePaolo D. J. (1988) Diagenesis and Sr isotopic evolution of seawater using data from DSDP 590B and 575. *Earth Planet. Sci. Lett.* **90**, 382–394.

Richter F. M. and Liang Y. (1993) The rate and consequences of Sr diagenesis in deep-sea carbonates. *Earth Planet. Sci. Lett.* **117**, 553–565.

Romanek C. S., Grossman E. L. and Morse J. W. (1992) Carbon isotopic fractionation in synthetic aragonite and calcite: effects of temperature and precipitation rate. *Geochim. Cosmochim. Acta* **56**, 419–430.

Santrock J., Studley S. A. and Hayes J. (1985) Isotopic analyses based on the mass spectra of carbon dioxide. *Anal. Chem.* **57**, 1444–1448.

Schauble E. A., Ghosh P. and Eiler J. M. (2006) Preferential formation of ^{13}C–^{18}O bonds in carbonate minerals, estimated using first-principles lattice dynamics. *Geochim. Cosmochim. Acta* **70**, 2510–2529.

Schauer A. J., Kelson J., Saenger C. and Huntington K. W. (2016) Choice of ^{17}O correction affects clumped isotope (Δ_{47}) values of CO_2 measured with mass spectrometry. *Rapid Commun. Mass Spectrom.* **30**, 2607–2616.

Schlanger S., Douglas R., Lancelot Y., Moore T. and Roth P. (1973) Fossil preservation and diagenesis of pelagic carbonates from the Magellan Rise, central North Pacific Ocean. *Init. Rep. Deep Sea Drilling Proj.* **17**, 407–427.

Schrag D. P. (1999) Effects of diagenesis on the isotopic record of late Paleogene tropical sea surface temperatures. *Chem. Geol.* **161**, 215–224.

Schrag D. P., DePaolo D. J. and Richter F. M. (1992) Oxygen isotope exchange in a two-layer model of oceanic crust. *Earth Planet. Sci. Lett.* **111**, 305–317.

Schrag D. P., DePaolo D. J. and Richter F. M. (1995) Reconstructing past sea surface temperatures: correcting for diagenesis of bulk marine carbonate. *Geochim. Cosmochim. Acta* **59**, 2265–2278.

Shackleton N. J. and Kennett J. P. (1975) Paleotemperature history of the Cenozoic and the initiation of Antarctic glaciation: oxygen and carbon isotope analyses in DSDP Sites 277, 279, and 281. *Init. Rep. Deep Sea Drilling Proj.* **29**, 743–755.

Shenton B. J., Grossman E. L., Passey B. H., Henkes G. A., Becker T. P., Laya J. C., Perez-Huerta A., Becker S. P. and Lawson M. (2015) Clumped isotope thermometry in deeply buried sedimentary carbonates: the effects of bond reordering and recrystallization. *Geol. Soc. Am. Bull.* **127**, 1036–1051.

Spooner P. T., Guo W., Robinson L. F., Thiagarajan N., Hendry K. R., Rosenheim B. E. and Leng M. J. (2016) Clumped isotope composition of cold-water corals: a role for vital effects? *Geochim. Cosmochim. Acta* **179**, 123–141.

Stax R. and Stein R. (1993) 34. Long-term changes in the accumulation of Organic Carbon in Neogene sediments, Ontong Java Plateau. In *Proceedings of the Ocean Drilling Program, Scientific Results*, vol. 30 (eds. W. Berger, L. Kroenke and L. Mayer), pp. 573–584.

Stolper D. A. and Eiler J. M. (2015) The kinetics of solid-state isotope-exchange reactions for clumped isotopes: a study of inorganic calcites and apatites from natural and experimental samples. *Am. J. Sci.* **315**, 363–411.

Stolper D. A. and Eiler J. M. (2016) Constraints on the formation and diagenesis of phosphorites using carbonate clumped isotopes. *Geochim. Cosmochim. Acta* **181**, 238–259.

Swart P., Burns S. and Leder J. (1991) Fractionation of the stable isotopes of oxygen and carbon in carbon dioxide during the reaction of calcite with phosphoric acid as a function of temperature and technique. *Chem. Geol.: Isotope Geosci. Sect.* **86**, 89–96.

Swart P. and Kennedy M. (2012) Does the global stratigraphic reproducibility of $\delta^{13}C$ in Neoproterozoic carbonates require a marine origin? A Pliocene-Pleistocene comparison. *Geology* **40**, 87–90.

Swart P. K. (2000) The oxygen isotopic composition of interstitial waters: evidence for fluid flow and recrystallization in the margin of the Great Bahama Bank. In *Proceedings of the Ocean Drilling Program, Scientific Results*, 166, pp. 91–98. Proceedings of the Ocean Drilling Program, Scientific Results.

Swart P. K. and Eberli G. (2005) The nature of the $\delta^{13}C$ of periplatform sediments: implications for stratigraphy and the global carbon cycle. *Sed. Geol.* **175**, 115–129.

Thiagarajan N., Adkins J. and Eiler J. (2011) Carbonate clumped isotope thermometry of deep-sea corals and implications for vital effects. *Geochim. Cosmochim. Acta* **75**, 4416–4425.

Thiagarajan N., Subhas A. V., Southon J. R., Eiler J. M. and Adkins J. F. (2014) Abrupt pre-Bolling-Allerod warming and circulation changes in the deep ocean. *Nature* **511**, 75–78.

Tripati A. K., Eagle R. A., Thiagarajan N., Gagnon A. C., Bauch H., Halloran P. R. and Eiler J. M. (2010) $^{13}C^{18}O$ isotope signatures and 'clumped isotope' thermometry in foraminifera and coccoliths. *Geochim. Cosmochim. Acta* **74**, 5697–5717.

Tripati A. K., Sahany S., Pittman D., Eagle R. A., Neelin J. D., Mitchell J. L. and Beaufort L. (2014) Modern and glacial tropical snowlines controlled by sea surface temperature and atmospheric mixing. *Nat. Geosci.* **7**, 205–209.

Urey H. C. (1947) The thermodynamic properties of isotopic substances. *J. Chem. Soc.*, 562–581.

Veizer J. and Mackenzie F. (2003) Evolution of sedimentary rocks. *Treatise Geochem.* **7**, 369–407.

Wacker U., Fiebig J., Tödter J., Schöne B. R., Bahr A., Friedrich O., Tütken T., Gischler E. and Joachimski M. M. (2014) Empirical calibration of the clumped isotope paleothermometer using calcites of various origins. *Geochim. Cosmochim. Acta* **141**, 127–144.

Wara M. W., Ravelo A. C. and Delaney M. L. (2005) Permanent El Niño-like conditions during the Pliocene warm period. *Science* **309**, 758–761.

Watkins J. and Hunt J. (2015) A process-based model for non-equilibrium clumped isotope effects in carbonates. *Earth Planet. Sci. Lett.* **432**, 152–165.

Watkins J. M., Hunt J. D., Ryerson F. J. and DePaolo D. J. (2014) The influence of temperature, pH, and growth rate on the $\delta^{18}O$ composition of inorganically precipitated calcite. *Earth Planet. Sci. Lett.* **404**, 332–343.

Watkins J. M., Nielsen L. C., Ryerson F. J. and DePaolo D. J. (2013) The influence of kinetics on the oxygen isotope composition of calcium carbonate. *Earth Planet. Sci. Lett.* **375**, 349–360.

Weiner S. and Dove P. M. (2003) An overview of biomineralization processes and the problem of the vital effect. *Rev. Mineral Geochem.* **54**, 1–29.

Wessel P., Smith W. H. F., Scharoo R., Luis F. and Wobbe F. (2013) Generic mapping tools: improved version released. *EOS Trans. AGU* **94**, 409–410.

Winkelstern I. Z. and Lohmann K. C. (2016) Shallow burial alteration of dolomite and limestone clumped isotope geochemistry. *Geology* **44**, 467–470.

Zaarur S., Affek H. P. and Brandon M. T. (2013) A revised calibration of the clumped isotope thermometer. *Earth Planet. Sci. Lett.* **382**, 47–57.

Zachos J., Pagani M., Sloan L., Thomas E. and Billups K. (2001) Trends, rhythms, and aberrations in global climate 65 Ma to present. *Science* **292**, 686–693.

Zeebe R. E. (1999) An explanation of the effect of seawater carbonate concentration on foraminiferal oxygen isotopes. *Geochim. Cosmochim. Acta* **63**, 2001–2007.

Zeebe R. E. and Wolf-Gladrow D. A. (2001) *CO_2 in Seawater: Equilibrium, Kinetics, Isotopes*. Gulf Professional Publishing.

Zhang Y. G., Pagani M. and Liu Z. (2014) A 12-million-year temperature history of the tropical Pacific Ocean. *Science* **344**, 84–87.

Associate Editor: Hagit P. Affek